A STUDY ON BUOYANCY DRIVEN FLOW OF CONDUCTING FLUID IN A VERTICAL MICRO-CHANNEL WITH HALL EFFECT

BY

PETER BUKAR MALGWI

DEPARTMENT OF MATHEMATICS,
FACULTY OF PHYSICAL SCIENCES,
AHMADU BELLO UNIVERSITY, ZARIA
NIGERIA.

October, 2017

A STUDY ON BUOYANCY DRIVEN FLOW OF CONDUCTING FLUID IN A VERTICAL MICRO-CHANNEL WITH HALL EFFECT

By

Peter Bukar MALGWI
B.Sc Mathematics (A.B.U., 2014)
P14SCMT8047

A DISSERTATION SUBMITTED TO THE SCHOOL OF POST GRADUATE STUDIES, AHMADU BELLO UNIVERSITY, ZARIA-NIGERIA, IN PARTIAL FULFILMENT FOR THE AWARD OF MASTERS DEGREE IN MATHEMATICS

DEPARTMENT OF MATHEMATICS, AHMADU BELLO UNIVERSITY, ZARIA, NIGERIA

October, 2017

DECLARATION

I declare that the work in this dissertation entitled "A STUDY ON BUOYANCY DRIVEN FLOW OF CONDUCTING FLUID IN A VERTICAL MICROCHANNEL WITH HALL EFFECT" has been carried out by me in the Department of Mathematics under the supervision of Prof. B. K. Jha and Prof. A. O. Ajibade. The information derived from the literature has been duly acknowledged in the text and a list of references provided. No part of this dissertation was previously presented for another degree or diploma at this or any institution.

MALGWI, Peter Bukar _____ _____

Signature Date

CERTIFICATION

This dissertation entitled A STUDY ON BUOYANCY DRIVEN FLOW OF CONDUCTING FLUID IN A VERTICAL MICROCHANNEL WITH HALL EFFECT by Peter Bukar MALGWI meets the regulations governing the award of the degree of Masters in Mathematics of the Ahmadu Bello University, and is approved for it's contribution to knowledge and literary presentation.

Prof. B. K. Jha	_____	_____
Chairman, Supervisory Committee	Signature	Date
Prof. A. O. Ajibade	_____	_____
Member, Supervisory Committee	Signature	Date
Prof. A. A. Tijjani	_____	_____
Head of Department	Signature	Date
_____	_____	_____
External Examiner	Signature	Date
Prof. S. Z. Abubakar	_____	_____
Dean, School of Postgraduate Studies	Signature	Date

DEDICATION

This dissertation is dedicated to God Almighty and my beloved parents Mr. and Mrs. Bukar Ali Malgwi.

ACKNOWLEDGEMENT

I am exceedingly grateful to God Almighty for giving me the wisdom and understanding to successfully complete this research work.

My sincere appreciation goes to my supervisor Prof. B. K. Jha for his fatherly advice, corrections, suggestion, insight and being a source of inspiration in this work. I am most grateful Sir, may God Almighty continue to preserve you and bring your heart desires to fulfilment.

My gratitude goes to my Minor supervisor Prof. A. O. Ajibade for his untold relentless effort in making suggestions, corrections and also reading the manuscript.

Special appreciation goes to Prof. A. A. Tijjani (Head of Department and also Dean Faculty of Physical Sciences), Dr. A.M. Ibrahim (Seminar Coordinator), Dr. H. M. Jibril (Postgraduate coordinator) and all academic and non-academic staff of the Department of Mathematics A.B.U Zaria for their contributions in various ways.

My heart felt thanks goes to my Dad and step mum Mr. and Mrs. Bukar Ali Malgwi for their prayers, financial support, and being a source of encouragement during this research work. To my sisters Sarah, Miriam, Palmata, Hyelhira, Rahila and lastly Joshua. I am indeed blessed to have you all.

i am grateful to God for the affirmation and support of my course mates and friends, Ashafa, Benjamin, Isaac, Simon, Ayodele, Umar, Micheal, Taiwo, Buchi, Jerry, Philemon, Joshua and many others. Thank you so much and remain ever blessed.

ABSTRACT

This dissertation presents a theoretical study on buoyancy driven flow of viscous, electrically conducting and incompressible fluid in a vertical micro-channel formed by two infinite vertical parallel plates in the presence of Hall effect. The problem is further extended to the case when the micro-channel plates are porous to investigate the effect of continuous suction/injection on the micro flow. Analytical solutions for energy and momentum equations are obtained using the method of undetermined coefficient. The influence of each governing parameter such as Hall current parameter, Hartmann number, suction/injection parameter, rarefaction parameter, fluid wall interaction parameter and wall-ambient temperature ratio on flow formation is analysed with the aid of line graphs and thereafter discussed. Numerical comparison of the present study with previously published results was established to validate the accuracy of the current solution. The results reveal that the Hall current parameter plays a significant role in enhancing the fluid flow, resulting to increase in fluid velocity and volume flow rate in both primary and secondary direction. In addition, it is interesting that the volume flow rate is higher in both flow directions due to increase in buoyancy force by increasing the temperature of the cooler wall. Also, the effect of the Hall current on velocity and volume flow could be further magnified by increasing gas rarefaction or increasing cooler wall temperature. Suction/injection on the other hand has a profound effect on the boundary layer thickness in which the suction reduces the thermal boundary layer thickness yielding a decrease in the convective current thereby decreasing fluid velocity and also the skin friction whereas injection thickens yielding an increase in fluid velocity.

TABLE OF CONTENTS

Flyleaf i

Title Page ii

Declaration iii

Certification iv

Dedication v

Acknowledgement vi

Abstract vii

Table of Contents viii

List of Figures x

NOMENCLATURE xvi

CHAPTER ONE

INTRODUCTION 1

1.1 General Introduction 1

1.2 Statement of the Problem 2

1.3 Significance of the study 2

1.4 Aim and Objectives 3

1.5 Research Methodology 3

1.6 Basic Definitions 4

CHAPTER TWO

LITERATURE REVIEW 7

2.1 Natural Convection in a Micro-Channel 7

2.2 Suction/Injection 8

2.3 Magnetohydrodynamics 8

2.4 Hall Effects 9

CHAPTER THREE

MATHEMATICAL MODELS 11

3.1 Hall Effect on MHD natural convection flow in a vertical micro-channel.(first case) 11

3.1.1 Dimensionless Analysis 13

3.1.2 Governing Equations in dimensionless form (first case) . 14

3.2 Fully developed MHD natural convection flow in a vertical micro-porous-channel with Hall effects (second case) 16

3.2.1 Dimensionless Analysis 17

3.2.2 Dimensionless form of problem (second case) 17

CHAPTER FOUR

RESULTS AND DISCUSSION 19

4.1 Hall Effect on MHD natural convection flow in a vertical micro-channel 19

4.2 Fully developed MHD natural convection flow in a vertical micro-porous-channel with Hall effects 33

CHAPTER FIVE

SUMMARY, CONCLUSION AND RECOMMENDATION 50

5.1 Summary 50

5.2 Conclusion 51

5.3 Recommendation 52

LIST OF FIGURES

4.1.1 Primary velocity profiles for different values of In when m=0.5, $\beta_v Kn = 0.05$, $M = 2$ 19

4.1.2 Secondary velocity profiles for different values of In when m=0.5, $\beta_v Kn = 0.05$, $M = 2$ 20

4.1.3 Primary velocity profiles for different values of $\beta_v Kn$, when $m = 0.5$, $In = 1.667$ and $M = 2$ 21

4.1.4 Secondary velocity profiles for different values of $\beta_v Kn$, when $m = 0.5$, $In = 1.667$ and $M = 2$ 21

4.1.5 Primary velocity profiles for different values of M when $\beta_v Kn = 0.05$, $m = 0.5$ and $In = 1.667$ 22

4.1.6 Secondary velocity profiles for different values of M when $\beta_v Kn = 0.05$, $m = 0.5$ and $In = 1.667$ 23

4.1.7 Primary velocity profiles for different values of m when $\beta_v Kn = 0.05$, $M = 2$ and $In = 1.667$ 24

4.1.8 Secondary velocity profiles for different values of m when $\beta_v Kn = 0.05$, $M = 2$ and $In = 1.667$ 24

4.1.9 Volume flow rate versus $\beta_v Kn$ for different values of M due to primary flow when $In = 0.5$, $m = 0.5$ 25

4.1.10 Volume flow rate versus $\beta_v Kn$ for different values of M due to secondary flow when $In = 0.5$, $m = 0.5$ 25

4.1.11 Volume flow rate versus $\beta_v Kn$ for different values of m due to primary flow when $M = 2$, $In = 1.667$ 26

4.1.12 Volume flow rate versus $\beta_v Kn$ for different values of m due to secondary flow when $M = 2$, $In = 1.667$ 26

4.1.13 Volume flow rate versus $\beta_v Kn$ for different values of In due to primary flow when $M = 2$, $m = 0.5$ 27

4.1.14 Volume flow rate versus $\beta_v Kn$ for different values of In due to secondary flow when $M = 2$, $m = 0.5$ 27
4.1.15 Variations of skin friction versus $\beta_v Kn$ for different values of In at $Y = 0$ due to primary flow when $M = 2$, $m = 0.5$ 27
4.1.16 Variations of skin friction versus $\beta_v Kn$ for different values of In at $Y = 0$ due to secondary flow when $M = 2$, $m = 0.5$ . . . 28
4.1.17 Variations of skin friction versus $\beta_v Kn$ for different values of In at $Y = 1$ due to primary flow when $M = 2$, $m = 0.5$ 28
4.1.18 Variations of skin friction versus $\beta_v Kn$ for different values of In at $Y = 1$ due to secondary flow when $M = 2$, $m = 0.5$ . . . 28
4.1.19 Variations of skin friction versus $\beta_v Kn$ for different values of m at $Y = 0$ due to primary flow when $M = 2$, $In = 1.667$ . . 29
4.1.20 Variations of skin friction versus $\beta_v Kn$ for different values of m at $Y = 0$ due to secondary flow when $M = 2$, $In = 1.667$. 29
4.1.21 Variations of skin friction versus $\beta_v Kn$ for different values of m at $Y = 1$ due to primary flow when $M = 2$, $In = 1.667$ . . 29
4.1.22 Variations of skin friction versus $\beta_v Kn$ for different values of m at $Y = 1$ due to secondary flow when $M = 2$, $In = 1.667$. 30
4.1.23 Variations of skin friction versus $\beta_v Kn$ for different values of M at $Y = 0$ due to primary flow when $m = 0.5$, $In = 1.667$. 30
4.1.24 Variations of skin friction versus $\beta_v Kn$ for different values of M at $Y = 0$ due to secondary flow when $m = 0.5$, $In = 1.667$ 30
4.1.25 Variations of skin friction versus $\beta_v Kn$ for different values of M at $Y = 1$ due to primary flow when $m = 0.5$,$In = 1.667$ . . 31
4.1.26 Variations of skin friction versus $\beta_v Kn$ for different values of M at $Y = 1$ due to secondary flow when $In = 1.667$, $m = 0.5$ 31
4.2.1 Primary velocity profiles for different values of $\beta_v Kn$ when $m = 0.5$, $S = 0.5$, $M = 2$ and $In = 1.667$ 33

4.2.2 Secondary velocity profiles for different values of $\beta_v Kn$ when $m = 0.5$, $S = 0.5$, $M = 2$ and $In = 1.667$ 34
4.2.3 Primary velocity profiles for different values of In when $\beta_v Kn = 0.05$, $m = 0.5$, $S = 0.5$, $M = 2$ 35
4.2.4 Secondary velocity profiles for different values of In when $\beta_v Kn = 0.05$, $m = 0.5$, $S = 0.5$, $M = 2$ 35
4.2.5 Primary velocity profiles for different values of Positive S (suction) when $\beta_v Kn = 0.05$, $m = 0.5$, $M = 2$, $In = 1.667$ 36
4.2.6 Primary velocity profiles for different values of negative S (injection) when $\beta_v Kn = 0.05$, $m = 0.5$, $M = 2$, $In = 1.667$ . . . 36
4.2.7 Secondary velocity profiles for different values of positive S (suction) when $\beta_v Kn = 0.05$, $m = 0.5$, $M = 2$, $In = 1.667$ . . 37
4.2.8 Secondary velocity profiles for different values of negative S (injection) when $\beta_v Kn = 0.05$, $m = 0.5$, $M = 2$, $In = 1.667$. 37
4.2.9 Primary velocity profiles for different values of M when $\beta_v Kn = 0.05$, $m = 0.5$, and $In = 1.667$ and $S = 0.5$ 38
4.2.10 Secondary velocity profiles for different values of M when $\beta_v Kn = 0.05$, $m = 0.5$, $In = 1.667$ and $S = 0.5$ 38
4.2.11 Primary velocity profiles for different values of m when $\beta_v Kn = 0.05$, $M = 2$, $In = 1.667$ and $S = 0.5$ 39
4.2.12 Secondary velocity profiles for different values of m when $\beta_v Kn = 0.05$, $M = 2$ and $S = 0.5$ and $In = 1.667$ 40
4.2.13 Volume flow rate versus $\beta_v Kn$ for different values of M when $m = 0.5$, $S = 0.5$ and $In = 1.667$ due to primary flow 40
4.2.14 Volume flow rate versus $\beta_v Kn$ for different values of M when $m = 0.5$, $S = 0.5$ and $In = 1.667$ due to secondary flow 41
4.2.15 Volume flow rate versus $\beta_v Kn$ for different values of m when $M = 2$, $S = 0.5$ and $In = 1.667$ due to primary flow 41

4.2.16 Volume flow rate versus $\beta_v Kn$ for different values of m when $M = 2$, $S = 0.5$ and $In = 1.667$ due to secondary flow 42
4.2.17 Volume flow rate versus $\beta_v Kn$ for different values of In when $M = 2$, $S = 0.5$ and $m = 0.5$ due to primary flow 42
4.2.18 Volume flow rate versus $\beta_v Kn$ for different values of In when $M = 2$, $S = 0.5$ and $m = 0.5$ due to secondary flow 42
4.2.19 Volume flow rate versus $\beta_v Kn$ for different values of S when $M = 2$, $In = 1.667$ and $m = 0.5$ due to primary flow 43
4.2.20 Volume flow rate versus $\beta_v Kn$ for different values of S when $M = 2$, $In = 1.667$ and $m = 0.5$ due to secondary flow 43
4.2.21 Variations of skin friction versus $\beta_v Kn$ for different values of M at $Y = 0$ due to primary flow when $In = 1.667$, $m = 0.5$,$S = 0.5$ 43
4.2.22 Variations of skin friction versus $\beta_v Kn$ for different values of M at $Y = 0$ due to secondary flow when $In = 1.667$, $m = 0.5$,$S = 0.5$ 44
4.2.23 Variations of skin friction versus $\beta_v Kn$ for different values of M at $Y = 1$ due to primary flow when $In = 1.667$, $m = 0.5$,$S = 0.5$ 44
4.2.24 Variations of skin friction versus $\beta_v Kn$ for different values of M at $Y = 1$ due to secondary flow when $In = 1.667$, $m = 0.5$,$S = 0.5$ 44
4.2.25 Variations of skin friction versus $\beta_v Kn$ for different values of In at $Y = 0$ due to primary flow when $M = 2$, $m = 0.5$,$S = 0.5$ 45
4.2.26 Variations of skin friction versus $\beta_v Kn$ for different values of In at $Y = 0$ due to secondary flow when $M = 2$, $m = 0.5$,$S = 0.5$ 45
4.2.27 Variations of skin friction versus $\beta_v Kn$ for different values of In at $Y = 1$ due to primary flow when $M = 2$, $m = 0.5$,$S = 0.5$ 45

4.2.28 Variations of skin friction versus $\beta_v Kn$ for different values of In at $Y = 1$ due to secondary flow when $M = 2$, $m = 0.5$, $S = 0.5$ 46
4.2.29 Variations of skin friction versus $\beta_v Kn$ for different values of m at $Y = 0$ due to primary flow when $M = 2$, $In = 1.667$, $S = 0.5$ 46
4.2.30 Variations of skin friction versus $\beta_v Kn$ for different values of m at $Y = 0$ due to secondary flow when $M = 2$, $In = 1.667$, $S = 0.5$ 47
4.2.31 Variations of skin friction versus $\beta_v Kn$ for different values of m at $Y = 1$ due to primary flow when $M = 2$, $In = 1.667$,$S = 0.5$ 47
4.2.32 Variations of skin friction versus $\beta_v Kn$ for different values of m at $Y = 1$ due to secondary flow when $M = 2$, $In = 1.667$, $S = 0.5$ 47
4.2.33 Variations of skin friction versus $\beta_v Kn$ for different values of S at $Y = 0$ due to primary flow when $M = 2$, $In = 1.667$, $m = 0.5$ 48
4.2.34 Variations of skin friction versus $\beta_v Kn$ for different values of S at $Y = 0$ due to secondary flow when $M = 2$, $In = 1.667$, $m = 0.5$ 48
4.2.35 Variations of skin friction versus $\beta_v Kn$ for different values of S at $Y = 1$ due to primary flow when $M = 2$, $In = 1.667$, $m = 0.5$ 48
4.2.36 Variations of skin friction versus $\beta_v Kn$ for different values of S at $Y = 1$ due to secondary flow when $M = 2$, $In = 1.667$, $m = 0.5$ 49

LIST OF TABLES

4.1 Numerical comparison of the values of the primary velocity (U) obtained in the present work with those of Chen and Weng (2005) and Jha *et al.* (2015) 32

4.2 Numerical comparison of the values of the primary velocity (U) obtained in the present work with Jha *et al.* (2015b) . . . 49

NOMENCLATURE

b	channel width
C_p, C_v	specific heat at constant pressure and volume, respectively
g	acceleration due to gravity
H_0	constant magnetic flux density
f_v, f_t	thermal and tangential momentum accommodation coefficient respectively
In	fluid-wall interaction parameter $\frac{\beta_t}{\beta_v}$
Kn	Knudsen number $\frac{\lambda}{b}$
m	Hall current parameter
M	Hartmann number
Pr	Prandtl number
u	velocity in the x-direction
w	velocity in the z-direction
Q	dimensionless complex velocity
Θ	dimensionless temperature
T	temperature of the fluid
S	suction/injection parameter
T_1	temperature of the right plate ($y = b$)
T_2	temperature of the left plate ($y = 0$)
n_e	number density of the electron
p_e	electron pressure

GREEK LETTERS

δ	dimensionless volume flow rate
β	coefficient of thermal expansion
β_t, β_v	dimensionless variables
γ_s	ratio of specific heat $\frac{C_p}{c_v}$
σ	electrical conductivity of the fluid
μ_e	magnetic permeability
ν	fluid kinematic viscosity
λ	molecular mean free path
k	thermal conductivity
ξ	wall ambient temperature
ρ	density
σ_t, σ_v	thermal and tangential accommodation coefficients, respectively
ω_e	cyclotron frequency
τ_e	electron collision time

CHAPTER ONE

INTRODUCTION

1.1 General Introduction

Fluid flow induced by temperature gradients commonly called natural or free convection has continued to attract a lot of attention from scientist and researchers recently, due to its practical applications in many geophysical and industrial/engineering applications. These include cooling of nuclear reactors, the boundary layer control in aerodynamics, crystal growth, food processing and cooling towers, thermal-energy storage system, crude oil extraction, and cores of nuclear reactors. Convection is also seen to play an important role in our weather system, oceanic currents, and sea-wind formation. In engineering applications, convection is commonly visualized in the formation of microstructures during the cooling of molten metals, and fluid flow around shrouded heat-dissipation fins, and solar ponds. A very common industrial application of natural convection is free air cooling without the aid of fans.
Natural convection through microchannels is gaining more interest recently. This is due to the fact that, as the size of the devices decrease, as in electronic devices, the amount of heat that needs to be dissipated per unit area increases. The performance of these devices is directly related to the temperature; therefore, it is highly desirable to understand the fluid flow and the heat transfer characteristics of buoyancy-induced microheat exchangers and micropump in microfluidic and thermal systems.

1.2 Statement of the Problem

Analysis for the fully developed natural convection in an open-ended vertical parallel-plate microchannel with asymmetric wall temperature distributions was investigated by Chen and Weng (2005) where they assumed the fluid to be viscous incompressible but electrically non-conducting. This result was extended by Jha *et al* (2015) by subjecting the flow under an applied transverse magnetic field and neglecting the influence of the Hall current. However, if the fluid considered is an ionized gas with low density, the electrical conductivity of the fluid becomes tensor if the influence of the electromagnetic fields becomes very strong yielding an effect known as the Hall current, in a direction normal to both the electric and magnetic field. This dissertation will therefore fill the observed vacuum in Jha *et al.* (2015) and Chen and Weng (2005) by considering the fluid to be electrically conducting and also incorporating the influence of the Hall currents by assuming the effect of the transversely applied magnetic field to be strong. This dissertation will further consider the role of suction/injection on the hydrodynamic behavior on the micro-fluidic flow.

1.3 Significance of the study

This research work derived and presented an analytical solution for buoyancy driven flow of conducting fluid in a vertical micro-channel with Hall effect subject to symmetric/asymmetric wall heating conditions. This research work is applicable in cooling device in computer microchips, Microelectromechanical system (MEMS), micro heat exchangers, micropump, microfuel cells, Hall accelerators, Hall sensors etc. Further, it is hoped that the results obtained will not only provide useful information for industrial or engineering applications but also serve as an improvement on the previous studies related to such flows.

1.4 Aim and Objectives

The aim of this work is to carry out an analytical study on buoyancy driven flow of viscous and electrically conducting fluid in a vertical micro-channel/micro-porous channel in presence of Hall Effect.
This aim will be achieved through the following objectives: To;

i examine the effect of varying the Hall current parameter on fluid velocity, skin-friction and volume flow rate on micro-channel/micro-porous channel flow behavior.

ii investigate the impact of suction/injection on fluid velocity, skin-friction and volume flow rate on micro-porous channel flow formation.

iii examine the effect of externally applied transverse magnetic field on natural convection flow in both microchannel and micro-porous channel.

iv investigate fluid flow behavior for different micro-channel dimensions dictated by $\beta_v Kn$

1.5 Research Methodology

To attain the above set objectives, we review existing literatures on natural convection flow in a micro-channel under different physical situations. Solution to the governing momentum and energy equations is presented analytically using the method of undetermined coefficient for both problems. Using a computer package, MATLAB (R2012b), the results obtained is presented graphically to investigate the influence of each governing parameter. Numerical comparison of the result obtained and previously published results is presented to establish the accuracy of the current solution.

1.6 Basic Definitions

1. **Compressible and incompressible fluid**: A compressible flow is a flow which the fluid density varies significantly within the flow field. While in an incompressible flow the density does not vary within he flow field.

2. **Free or Natural Convection**: Free or Natural convection is a mechanism in which fluid motion is generated only by density differences in fluid cause by temperature gradients. It is a type of heat transport in which the fluid motion is not generated by an external source (pump, fan, suction devices).

3. **Conducting and non-conducting fluid**: Materials that conducts electricity have free ions (charged particle) thus there is flow of current while Materials that do not have free ions (charged particle) to help in the flow of current are known as Non-conducting fluid.

4. **Boussinessq approximation**: Boussinessq approximation is the assumption that the fluid flow is considered under little variations of temperature and density.

5. **Skin friction**: Is a component of drag, the force resisting the motion of a solid body through a fluid. It arises from the friction of the fluid against the skin of the object that is moving through it. Skin friction follows the drag equation and rises with the square of the velocity. Skin friction can be reduced by shaping the moving body so that smooth flow is possible.

6. **Injection**: Is a force that causes a fluid to be drawn out of an interior space or to adhere to a surface because of the difference between the external and internal pressures.

7. **Suction**: Is a force that causes a fluid to be drawn into an interior space or to adhere to a surface because of the difference between the external and internal pressures

8. **Symmetric/asymmetric heating**: This is a type of heating of the boundary layers in which equal/unequal amount of constant heating is applied on boundary surfaces of the system.

9. **Dimensionless quantity**: is a quantity without an associated physical dimension.

10. **Magnetic field**: is the magnetic effect of electric currents and magnetic material.

11. **MHD**: Implies Magnetohydrodynamics which is the study of the interaction between electric and magnetic forces in a flow. Since the magnetohydrodynamic equations combine the full complexity of Maxwell's equations with the fluid dynamics equations, it is clear that they will be extremely difficult to solve in their general form. However, by adopting some approximations, the general equations are simplified. these are:
    Maxwell's equations:

$$\nabla \times E = \frac{\partial B}{\partial t}$$
$$\nabla \times B = \mu_0 j$$
$$\nabla \bullet B = 0$$
$$K_0 \nabla \bullet E = \rho_e$$

    Conservation of mass:

$$\frac{\partial \rho}{\partial t} + \nabla \bullet (\rho v) = 0$$

    Equation of motion:

$$\rho \frac{Dv}{Dt} = -\nabla p + \mu \nabla^2 v + \psi + j \times B$$

Conservation of energy:

$$\rho\left(\frac{De}{Dt}+\frac{1}{2}\frac{Dv^2}{Dt}\right)=E\bullet j+\nabla\bullet(K\nabla T)-\sum_s\nabla\bullet(V_s\rho_s h_s)-\nabla\bullet(pv)+\phi$$

12. **Hall Effect**: is the production of a voltage difference across an electrical conductor, transverse to an electric current in the conductor and a magnetic field perpendicular to the current.

    From the generalised Ohms law in which ion slip and and pressure diffusion effects are neglected,

    $$j=\sigma[E+v\times B-\beta(j\times B)]$$

    where $\beta=\frac{1}{n_e e}$, $\sigma=n_e e^2\tau/m_e$

    since the electrical conductivity in compressible gaseous plasmas are not not constant, the above expression can be written as follows:

    $$j_x=\frac{\sigma}{1+(\omega\tau)^2}[E_x-\omega\tau(E_y-UB)]$$

    $$j_y=\frac{\sigma}{1+(\omega\tau)^2}[E_y-UB+\omega\tau E_x]$$

    where $\sigma\beta B=\omega\tau$. From the above we observe that as a consequence of the Hall effect, axial current can flow

13. **Microchannel**: is a channel with hydraulic diameter below $1mm$.

CHAPTER TWO

LITERATURE REVIEW

2.1 Natural Convection in a Micro-Channel

Micro-scale flow formation and heat transfer has of recent received intensive interest in the field of science and technology due to the emergence of micro-electromechanical systems technology (MEMS). When the mean free path of the fluid is comparable to the channel's characteristic dimension, the continuum assumption is no longer valid and velocity slip and temperature jump may occur at the micro channel surfaces. Chen and Weng (2005) discussed the flow formation of steady fully developed natural convection flow in a vertical micro channel formed by two infinite vertical parallel plates due to asymmetric heating of micro channel walls. The effects of rarefaction and fluid-wall interaction were shown to enhance the volume flow rate and to reduce the rate of heat transfer. This result was further extended by taking into account suction/injection on the microchannel walls by Jha *et al.* (2014). Their results showed that skin-friction as well as rate of heat transfer strongly depends on the suction/injection parameter. Numerical solutions were obtained by Buonomo and Manca (2012) for natural convection in parallel-plate vertical microchannels due to asymmetric heating by imposing constant heat flux on the boundaries. The same authors (2012) further performed a numerical study on transient mixed convection in a vertical microchannel that is asymmetrically or symmetrically heated at uniform heat fluxes. The transient hydrodynamics and thermal behaviours of fluid flow in an open-ended vertical parallel-plate microhannel, under the effect of the hyperbolic-heat-conduction model, were investigated semi-analytically in (2007). In recent past, the work of Chen and Weng (2007) was extended to mixed convection by Avci and Adyin (2007). Avci and Aydin (2009) conducted a study on fully developed mixed convective

flow in a vertical micro-annulus formed by two concentric micro-tubes.

2.2 Suction/Injection

Suction or injection plays an important role in the control of flow past an infinite plate or micro-channel, hence its importance in practical problem involving film cooling, geophysical, biomedical, engineering and environmental applications. The significance of suction/injection on the boundary layer control in the field of aerodynamics and space science was emphasized by Singh (1984). Jha *et al.* (2014) investigated on natural convection flow in vertical micro-porous channel. In a related work, Jha and Aina (2014) further extended the work of Avci and Aydin (2009) to the case when the vertical micro-annulus formed by two concentric micro-tubes are porous, i.e. where there is suction or injection through the annulus surfaces. They concluded in their study that as suction/injection on the micro-porous-annulus (MPA) increases, the fluid velocity and temperature increase.

2.3 Magnetohydrodynamics

Magnetohydrodynamic (MHD) phenomenon has attracted the attention of engineers and scientists in recent past owing to its relevance in MHD accelerators, electric transformers, cooling of a metallic plate in a cooling bath are just some examples of realistic applications. Magnetohydrodynamic (MHD) natural convection flow of different fluids over different geometries has been studied widely in the literature. Despite the fact that there are numerous studies on natural convection flow of an electrically conducting fluid in channels, there are just a few studies regarding MHD natural convection flow of an electrically

conducting fluid in microchannel. For example, Jha *et al.* (2015) studied the fully developed natural convection flow of conducting fluid in a vertical parallel plate microchannel in the presence of transverse magnetic field. They reported that, increase in Hartmann number is responsible for reduction in the volume flow rate. The combined impact of externally applied transverse magnetic field and suction/injection on steady natural convection flow of conducting fluid in a vertical microchannel was carried out by Jha *et al.* (2015) In another work, Jha *et al.* (2015) investigated the role of wall surface curvature on transient MHD free convective flow in vertical micro-concentric-annuli. Jha *et al.* (2015) investigated the exact solution of steady fully developed natural convection flow of viscous, incompressible, and electrically conducting fluid in a vertical annular microchannel. Also, Jha and Aina (2016) presented the MHD natural convection flow in a vertical micro-porous-annulus (MPA) in the presence of radial magnetic field. The MHD natural convection flow in vertical micro-concentric-annuli (MCA) in the presence of radial magnetic field has been discussed by Jha *et al.* (2016). Meanwhile, the above mentioned works considered convective flow of rarefield fluid and hence both walls have the same velocity slip and temperature jump. Velocity slip and temperature jump are known to depend on the Knudsen number and the thermal and tangential momentum accommodation coefficients, representing the effects of rarefaction and fluid wall interaction. These coefficients are properties of the fluid, thermal conditions of the flow, as well as the material and quality of the channel walls.

2.4 Hall Effects

In partially ionized gases, the phenomenon of Hall effects occurs when the strength of the impressed magnetic field is very strong or when the cyclotron

frequency is high (Sutton and Sherman, (1965). The current induced in a fluid is usually carried predominantly by electrons, which undergo successive collisions with other charged or neutral particles and are usually more mobile than ions. As a result of these gyration and drift of charged particles, the conductivity parallel to the electric field is reduced and the current is induced in the direction normal to both electric and magnetic fields. This phenomenon is known as the Hall effects. Singh (1984) investigated the effect of the Hall current on the natural convection flow of a viscous, incompressible and electrically conducting fluid past an accelerated vertical porous plate. Jha and Apere (2010) studied the effect of Hall and ion-slip currents on the unsteady MHD Couette flows of a viscous, incompressible and electrically conducting fluid between two parallel porous plates in a rotating system when the lower plate has been impulsively started. They concluded that the influence of the Hall and ion slip parameters have a reducing effect on the magnitude of the secondary velocity especially when the magnetic lines of force are fixed relative to the moving plate. In another work, Jha and Apere (2011) extended their work (2010) for the case of porous plate. Seth and Singh (2015) studied the mixed convection flow in a rotating channel with Hall and wall conductance effects. Ghosh and Bhattacharjee (2000) investigated the hydromagnetic steady flow of a Newtonian fluid passing through a rotating channel with Hall effects.

CHAPTER THREE

MATHEMATICAL MODELS

3.1 Hall Effect on MHD natural convection flow in a vertical micro-channel.(first case)

The geometry of the system under consideration in this present study is shown schematically in Figure 1. Consider the fully developed natural convection flow of a viscous, incompressible and electrically conducting fluid in a vertical microchannel formed by two infinite vertical parallel plates under the influence of Hall effect. The plates are heated asymmetrically with one plate maintained at a temperature T_1 while the other plate at a temperature T_2 where $T_1 > T_2$. Due to temperature gradient between the plates, natural convection flow occurs in the microchannel. A uniform magnetic field H_0 is applied in the direction perpendicular to the direction of flow and neglecting the induced magnetic fields by assuming a very small magnetic Reynolds number. The effect of Hall current is taken into consideration which gives rise to velocity in the transverse direction. Hence, $\bar{V}$ is given by $(u, 0, w)$. The flow is assumed to be steady and fully developed. Following Jha et al. (2015) and considering Hall effects, under Boussinesq's approximation, the governing equations for the present physical situation are given as:

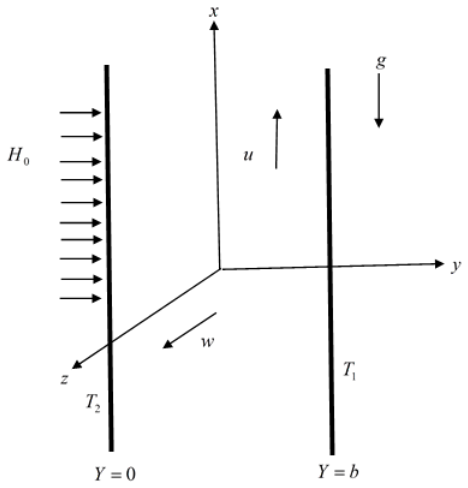


Figure 1: Schematic diagram of the flow domain

For steady motion, the Maxwell equations and Ohm's law taking Hall current into account in the absence of electric field, (Cowling, 1957) are given by:

$$\nabla \cdot \bar{B} = 0 \tag{3.1.1}$$

$$\nabla \times \bar{H} = \bar{J} \tag{3.1.2}$$

$$\nabla \cdot \bar{J} = 0 \tag{3.1.3}$$

$$\bar{J} + \frac{\bar{J} \times \bar{H}}{H_0} m = \sigma(\mu_e V \times \bar{H} + \frac{1}{en_e} \nabla p_e) \tag{3.1.4}$$

where $\bar{J} = J_x \hat{i} + J_z \hat{k}$ is the electric density along primary and transverse direction, $m = \omega_e \tau_e$ is the Hall parameter

under the usual assumptions that the electron pressure (weakly ionised gas), the thermoelectric pressure and ion slip are negligible, Eqn. (3.1.4) yields:

$$J_z = \frac{\sigma \mu_e H_0}{1 + m^2}(u + mw) \tag{3.1.5}$$

$$J_x = \frac{\sigma \mu_e H_0}{1 + m^2}(mu - w) \tag{3.1.6}$$

within the framework of these assumptions, the equations which govern the buoyancy induced flow of an electrically conducting fluid are:

$$\nu\frac{d^2u}{dy^2} + g\beta(T - T_0) - \frac{\sigma H_0^2\mu_e^2}{\rho}\left(\frac{u + mw}{1 + m^2}\right) = 0 \tag{3.1.7}$$

$$\nu\frac{d^2w}{dy^2} + \frac{\sigma H_0^2\mu_e^2}{\rho}\left(\frac{mu - w}{1 + m^2}\right) = 0 \tag{3.1.8}$$

$$\frac{d^2T}{dy^2} = 0 \tag{3.1.9}$$

with momentum and thermal boundary conditions:

$$T = T_2 + \frac{2 - f_t}{f_t}\frac{2\gamma_s}{\gamma_s + 1}\frac{\lambda}{Pr}\frac{dT}{dy}|_{y=0}$$

$$T = T_1 - \frac{2 - f_t}{f_t}\frac{2\gamma_s}{\gamma_s + 1}\frac{\lambda}{Pr}\frac{dT}{dy}|_{y=b}$$

$$u = \frac{2 - f_v}{f_v}\lambda\frac{du}{dy}|_{y=0}, \qquad w = \frac{2 - f_v}{f_v}\lambda\frac{dw}{dy}|_{y=0} \tag{3.1.10}$$

$$u = -\frac{2 - f_v}{f_v}\lambda\frac{du}{dy}|_{y=b}, \qquad w = -\frac{2 - f_v}{f_v}\lambda\frac{dw}{dy}|_{y=b}$$

3.1.1 Dimensionless Analysis

Introducing the following dimensionless quantities:

$$Y = \frac{y}{b}, M = \frac{\sigma\mu_e^2 H_0^2 b^2}{\rho\nu}, (U, W) = \frac{(u, w)\nu}{g\beta\Delta T b^2},$$

$$\Delta T = T_1 - T_0, \Theta = \frac{T - T_0}{\Delta T}, m = \omega_e\tau_e$$

$$\beta_v = \frac{2 - f_v}{f_v}, \beta_t = \frac{2 - f_t}{f_t}\frac{2\gamma_s}{\gamma_s + 1}\frac{1}{Pr}, Kn = \frac{\lambda}{b}, ln = \frac{\beta_t}{\beta_v}, \xi = \frac{T_2 - T_0}{T_1 - T_0} \tag{3.1.11}$$

where m is the Hall current parameter, M is the Hartmann number, ρ is the fluid density, Pr is the Prandtl number as defined in the nomenclature.

3.1.2 Governing Equations in dimensionless form (first case)

Substituting the dimensionless parameters in $(3.1.7-3.1.9)$ above, the governing equations for the problem in dimensionless form are as follows:

$$\frac{d^2U}{dY^2} + \Theta - \frac{M}{(1+m^2)}(U + mW) = 0 \tag{3.1.12}$$

$$\frac{d^2W}{dY^2} + \frac{M}{(1+m^2)}(mU - W) = 0 \tag{3.1.13}$$

$$\frac{d^2\Theta}{dY^2} = 0 \tag{3.1.14}$$

If we define the complex velocity $Q = U + iW$, equations (3.1.12) and (3.1.13) can be combined to single equation:

$$\frac{d^2Q}{dY^2} + \Theta - M_1^2 Q = 0 \tag{3.1.15}$$

with the boundary conditions:

$$\Theta(0) = \xi + \beta_v Kn ln \frac{d\Theta}{dY}|_{Y=0}, \qquad \Theta(1) = 1 - \beta_v Kn ln \frac{d\Theta}{dY}|_{Y=1} \tag{3.1.16}$$

$$Q(0) = \beta_v Kn \frac{dQ}{dY}|_{Y=0}, \qquad Q(1) = -\beta_v Kn \frac{dQ}{dY}|_{Y=1} \tag{3.1.17}$$

where $M_1^2 = \frac{M}{1+im}$,

ξ is the fluid wall interaction parameter and $\beta_v Kn$ is the rarefaction parameter.

Solution to Eqns.$(3.1.14-3.1.15)$ subject to the boundary condition Eqns.$(3.1.16-3.17)$ yields:

$$\Theta(Y) = A_0 + A_1 Y \tag{3.1.18}$$

$$Q(Y) = C_1 \cosh(M_1 Y) + C_2 \sinh(M_1 Y) + \frac{1}{M_1^2}(A_0 + A_1 Y) \tag{3.1.19}$$

where A_0, A_1, C_1 and C_2 are defined in the appendix.

Two important parameters for buoyancy induced microflow and microheat transfer are the volume flow rate (δ) and Skin friction (τ), respectively. Considering the effects of the Hall current, the present analysis will capture the volume flow and also the skin friction in both the primary and secondary direction of flow.

Dimensionless volume flow is given by:

$$\delta = \int_0^1 Q(Y)dY \tag{3.1.20}$$

by using the expression for $Q(Y)$ in (3.1.19) above, the volume flow δ can be written as:

$$\delta = \frac{C_1}{M_1}\left(sinh(M_1)\right) + \frac{C_2}{M_1}\left(cosh(M_1) - 1\right) + \frac{1}{M_1^2}\left(A_0 + \frac{A_1}{2}\right) \tag{3.1.21}$$

where $Q_{x0} = \Re_e(\delta)$ and $Q_{z0} = Im(\delta)$

similarly, the skin friction on the micro-channel surfaces due to primary flow is given by $\tau_x = \Re_e(\frac{dQ}{dY})$, while skin friction due to secondary flow is defined $\tau_z = Im(\frac{dQ}{dY})$.

where

$$\frac{dQ}{dY}|_{Y=0} = M_1C_2 + \frac{A_1}{M_1^2}$$

$$\frac{dQ}{dY}|_{Y=1} = \frac{A_1}{M_1^2} - M_1(C_1sinh(M_1) + C_2cosh(M_1))$$

3.2 Fully developed MHD natural convection flow in a vertical micro-porous-channel with Hall effects (second case)

By extension using the same model above, we introduce suction/injection on the micro-channel surfaces. Diagram is shown in Figure 2.

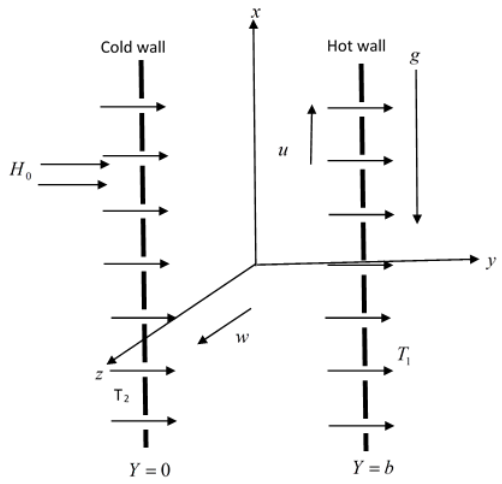


Figure 2: Schematic diagram of the flow domain (second case)

$$\nu\frac{d^2u}{dy^2} - V_0\frac{du}{dy} + g\beta(T - T_0) - \frac{\sigma\mu_e^2H_0^2}{\rho}\left(\frac{u + mw}{1 + m^2}\right) = 0 \tag{3.2.1}$$

$$\nu\frac{d^2w}{dy^2} - V_0\frac{dw}{dy} + \frac{\sigma\mu_e^2H_0^2}{\rho}\left(\frac{um - w}{1 + m^2}\right) = 0 \tag{3.2.2}$$

$$\alpha\frac{d^2T}{dy^2} - V_0\frac{dT}{dy} = 0 \tag{3.2.3}$$

with momentum and thermal boundary conditions:

$$T = T_2 + \frac{2 - f_t}{f_t}\frac{2\gamma_s}{\gamma_s + 1}\frac{\lambda}{Pr}\frac{dT}{dy}|_{y=0}$$

$$T = T_1 - \frac{2 - f_t}{f_t}\frac{2\gamma_s}{\gamma_s + 1}\frac{\lambda}{Pr}\frac{dT}{dy}|_{y=b} \tag{3.2.4}$$

$$u = \frac{2 - f_v}{f_v}\lambda\frac{du}{dy}|_{y=0}, \qquad w = \frac{2 - f_v}{f_v}\lambda\frac{dw}{dy}|_{y=0}$$

$$u = -\frac{2 - f_v}{f_v}\lambda\frac{du}{dy}|_{y=b}, \qquad w = -\frac{2 - f_v}{f_v}\lambda\frac{dw}{dy}|_{y=b}$$

3.2.1 Dimensionless Analysis

Introducing the following dimensionless quantities:

$$Y = \frac{y}{b}, M = \frac{\sigma \mu_e^2 H_0^2 b^2}{\rho \nu}, (U, W) = \frac{(u, w)\nu}{g\beta \Delta T b^2}$$

$$\Delta T = T_1 - T_0, S = \frac{V_0 b}{\nu}, Pr = \frac{\nu}{\alpha}, \Theta = \frac{T_1 - T_0}{\Delta T}, m = \omega_e \tau_e \tag{3.2.5}$$

$$\beta_v = \frac{2 - f_v}{f_v}, \beta_t = \frac{2 - f_t}{f_t} \frac{2\gamma_s}{\gamma_s + 1} \frac{1}{Pr}, Kn = \frac{\lambda}{b}, ln = \frac{\beta_t}{\beta_v}, \xi = \frac{T_2 - T_0}{T_1 - T_0}$$

3.2.2 Dimensionless form of problem (second case)

$$\frac{d^2U}{dY^2} - S\frac{dU}{dY} + \Theta - \frac{M}{1 + m^2}(U + mW) = 0 \tag{3.2.6}$$

$$\frac{d^2W}{dY^2} - S\frac{dW}{dY} + \frac{M}{1 + m^2}(mU - W) = 0 \tag{3.2.7}$$

$$\frac{d^2\Theta}{dY^2} - SPr\frac{d\Theta}{dY} = 0 \tag{3.2.8}$$

By defining the complex velocity $Q = U + iW$, equations (3.2.6) and (3.2.7) can be combined to single

$$\frac{d^2Q}{dY^2} - S\frac{dQ}{dY} + \Theta - M_1^2 Q = 0 \tag{3.2.9}$$

where $M_1^2 = \frac{M}{1+im}$

subject to the dimensionless thermal and momentum boundary condition:

$$\Theta(0) = \xi + \beta_v Knln\frac{d\Theta}{dY}|_{Y=0}, \Theta(1) = 1 - \beta_v Knln\frac{d\Theta}{dY}|_{Y=1} \tag{3.2.10}$$

$$Q(0) = \beta_v Kn\frac{dQ}{dY}|_{Y=0}, Q(1) = -\beta_v Kn\frac{dQ}{dY}|_{Y=1} \tag{3.2.11}$$

solution to Eqns.(3.2.8-3.2.9) subject to the boundary condition in Eqn(3.2.10-3.2.11) yields:

$$\Theta(Y) = A + Bexp(SPrY) \tag{3.2.12}$$

$$Q(Y) = C_1 exp(K_1 Y) + C_2 exp(K_2 Y) + \frac{A}{M_1^2} - B_0 exp(SPrY) \tag{3.2.13}$$

where A,B, C_1, C_2,K_1, K_2 and B_0 are defined in the appendix.

the volume flow δ and skin friction is obtained by using the expression:

$$\delta = \int_0^1 Q(Y) dY \tag{3.2.14}$$

by using Eqn.(3.2.13) the volume flow can be expressed as:

$$\delta = \frac{C_1}{K_1}\left(exp(K_1) - 1\right) + \frac{C_2}{K_2}\left(exp(K_2) - 1\right) + \frac{A}{M_1^2} - \frac{K_3}{SPr}\left(exp(SPr) - 1\right) \tag{3.2.15}$$

where $Q_{x0} = \Re(\delta)$ and $Q_{z0} = Im(\delta)$

similarly, the skin friction defined as τ_x and τ_z is obtained by differentiating Eqn.(3.2.13) as follows:

$$\frac{dQ}{dY}|_{Y=0} = C_1 K_1 + C_2 K_2 - K_3 SPr \tag{3.2.16}$$

$$\frac{dQ}{dY}|_{Y=1} = C_1 K_1 e^{K_1} + C_2 K_2 e^{K_2} - SPr K_3 exp SPr \tag{3.2.17}$$

where $\tau_{xk} = \Re(\frac{dQ}{dY})$ and $\tau_z k = Im(\frac{dQ}{dY})$ for $k = 0, 1$ indicating the boundary plates.

CHAPTER FOUR

RESULTS AND DISCUSSION

4.1 Hall Effect on MHD natural convection flow in a vertical micro-channel

This chapter presents the results obtained from the previous chapter in the form of line graphs that gives a proper insight of the discussion of the calculated results. The interactive effects of the Hall current parameter (m), Hartmann number (M), rarefaction parameter ($\beta_v Kn$), fluid wall interaction parameter (In) and the wall-ambient temperature ratio ξ under three cases ($\xi = 1$: two heating, $\xi = 0$: one heating and one not heating, $\xi = -1$: one heating and one cooling) on flow formation are investigated. The present study has been conducted over the interval $0 \leq m \leq 1.0$, $0 \leq M \leq 10$, $0 \leq \beta_v Kn \leq 0.1$ and $0 \leq In \leq 10$ with the selected reference values of $\beta_v Kn = 0.05$ and $In = 1.667$ as presented by Chen and Weng (2005).

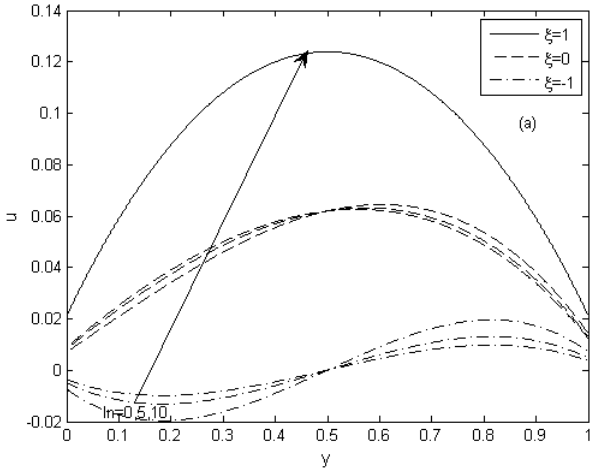


Figure 4.1.1: Primary velocity profiles for different values of In when m=0.5, $\beta_v Kn = 0.05$, $M = 2$

The expression for the temperature in equation (3.1.18), the effects of the rarefaction parameter $\beta_v Kn$ and fluid-wall interaction parameter In on the temperature profile and rate of heat transfer which is expressed as the Nusselt

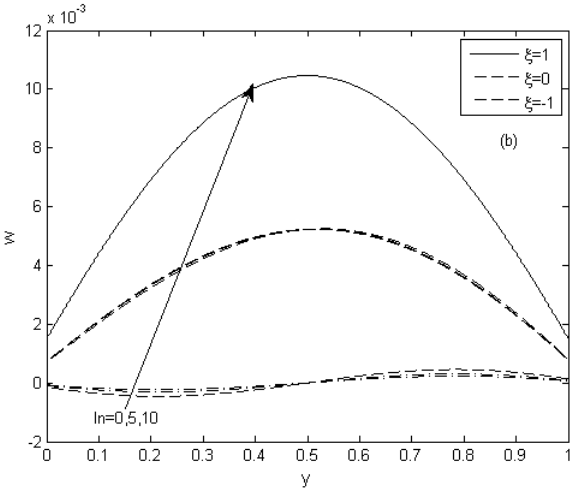


Figure 4.1.2: Secondary velocity profiles for different values of In when m=0.5, $\beta_v Kn = 0.05$, $M = 2$

number are exactly the same as those given by Chen and Weng (2005).

Figures 4.1.1 and 4.1.2 displays the effect of wall-ambient temperature difference ratio (ξ) as well as fluid wall interaction parameter (In) on the primary (U) and secondary velocity (W). It is clearly seen for both cases that, the role of the fluid wall interaction parameter is found to increase the fluid plate molecular interaction resulting to an asymmetric velocity distribution in both primary and secondary flow direction. Furthermore, the influences of fluid-wall interaction parameter on the microchannel slip velocity become significant with the decrease in the wall-ambient temperature difference ratio which is more pronounced in the case of primary velocity.

Figures 4.1.3 and 4.1.4 illustrates the effect of the rarefaction parameter ($\beta_v Kn$) as well as wall-ambient temperature difference ratio (ξ) on the primary and secondary velocity. It is observed for both primary and secondary velocity that, increasing the wall-ambient temperature difference ratio as well as rarefaction parameter leads to enhancement in the fluid velocity and velocity slip. For asymmetric heating $\xi = -1$ however, corresponding to the physical situation when one of the plates is heated and the other cooled, considers two buoyancy driven flows of the same magnitude but different direction as a result, the net flow is observed to be zero. These effects are more pronounced in

the case of secondary velocity. This result yields an observable increase in the fluid velocity. This physical phenomenon can also be explained from the fact that, as rarefaction parameter increases, the temperature jump increases and this reduces the amount of heat transfer from the microchannel surfaces to the fluid. The reduction in fluid velocity due to the reduction in heat transfer is offset by the increase in the fluid velocity due to the reduction in the frictional retarding forces near the microchannel surfaces.

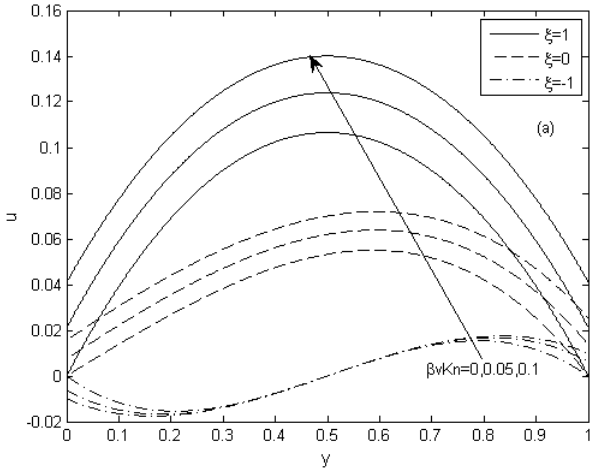


Figure 4.1.3: Primary velocity profiles for different values of $\beta_v Kn$, when $m = 0.5$, $In = 1.667$ and $M = 2$

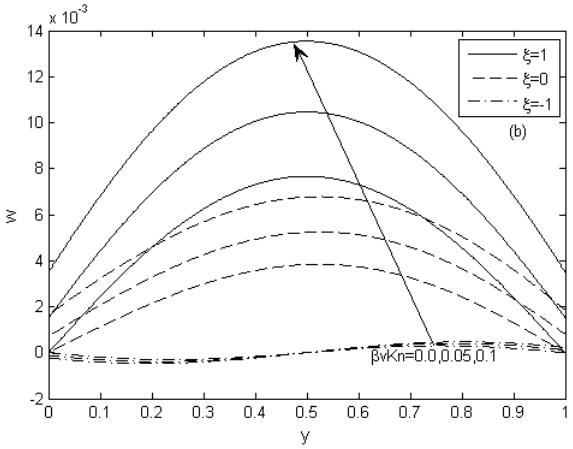


Figure 4.1.4: Secondary velocity profiles for different values of $\beta_v Kn$, when $m = 0.5$, $In = 1.667$ and $M = 2$

Figures 4.1.5 and 4.1.6 display the combined effects of the Hartmann number (M) and wall-ambient temperature difference ratio (ξ) on the primary and

secondary velocity profiles. It is seen in the case of primary velocity that, increasing the values of Hartmann number have a tendency to slow down the movement of the fluid in the microchannel while the reverse trend occurs in the case of secondary velocity. This is due to the fact that the application of magnetic field creates a resistive force similar to the drag force that acts in the opposite direction of the fluid motion, thus causing the fluid velocity to decreases. Meanwhile, the influence of Hartmann number on the microchannel slip velocity becomes significant with the increase of the wall-ambient temperature difference ratio.

Figures 4.1.7 and 4.1.8 shows the effects of the Hall current parameter (m) as well as wall-ambient temperature difference ratio (ξ) on the primary and secondary velocity. It is evident for both primary and secondary velocity that, increasing the Hall current parameter leads to increase in the fluid velocity. Furthermore, an increase in the Hall current parameter, decreases the reducing effect of the magnetic field on the complex velocity Q, thereby increasing the velocity in both primary and secondary velocity.

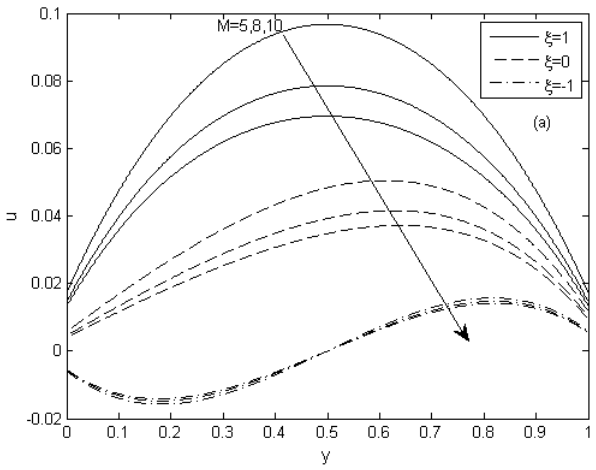


Figure 4.1.5: Primary velocity profiles for different values of M when $\beta_v Kn = 0.05$, $m = 0.5$ and $In = 1.667$

Figures 4.1.9 and 4.4.10 illustrates the effects of rarefaction parameter, Hartmann number and wall-ambient temperature difference ratio (ξ) on volume flow rate. It is observed in the case of primary volume flow rate that, increase

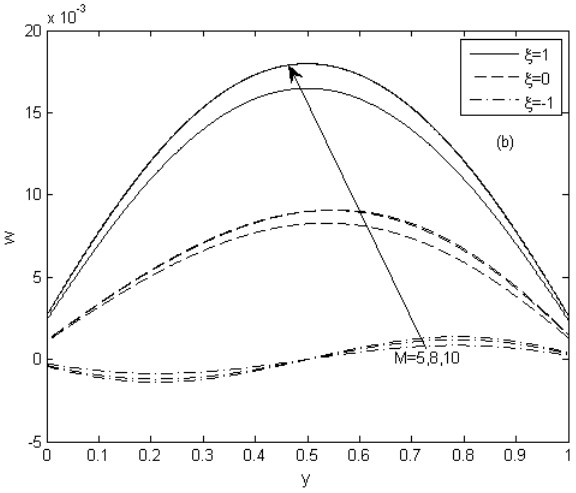


Figure 4.1.6: Secondary velocity profiles for different values of M when $\beta_v Kn = 0.05$, $m = 0.5$ and $In = 1.667$

in Hartmann number cause a reduction in volume flow rate. This may be attributed to the fact that, fluid velocity decreases as the Hartmann number increases, which cause a reduction in the volume flow rate while the reverse trend occurs in the case of secondary volume flow rate.

The volume flow rate variations are shown in Figures 4.1.11 and 4.1.12 with respect to Hall current parameter and rarefaction parameter for different values of wall-ambient temperature difference ratio. It is seen for both cases that, an increase in rarefaction parameter leads to enhancement in volume flow rate. Furthermore, it is evident that volume flow rate is found to be increasing function of Hall current parameter.

Figures 4.1.13 and 4.1.14 exhibit the effects of rarefaction parameter and fluid wall interaction parameter on the volume flow rate for different values of wall-ambient temperature difference ratio. It is seen for both primary and secondary volume flow rate, the increase in rarefaction parameter leads to increase in volume flow rate. Furthermore, it is evident that volume flow rate is found to be increasing function of fluid wall interaction as well as wall-ambient temperature difference ratio.

Figures 4.1.15−4.1.16 and 4.1.17−4.1.18 presents the effect of rarefaction, fluid

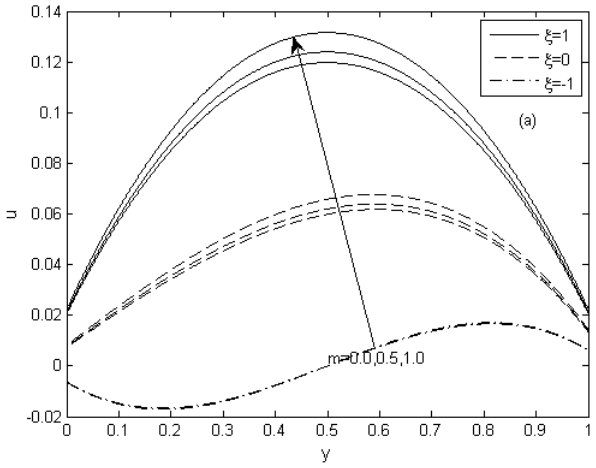


Figure 4.1.7: Primary velocity profiles for different values of m when $\beta_v Kn = 0.05$, $M = 2$ and $In = 1.667$

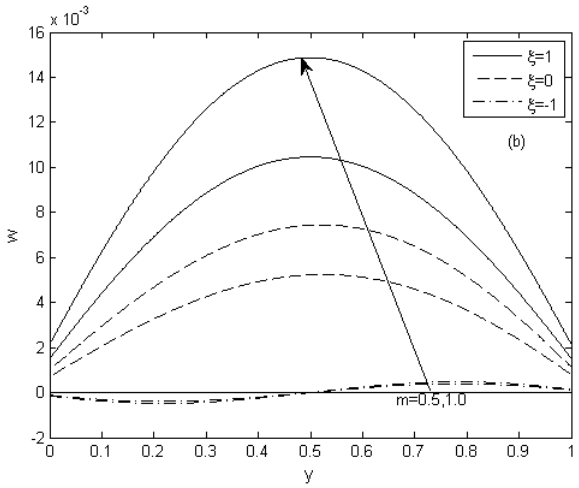


Figure 4.1.8: Secondary velocity profiles for different values of m when $\beta_v Kn = 0.05$, $M = 2$ and $In = 1.667$

wall interaction parameter as well as wall-ambient temperature difference ratio on the skin friction at the microchannel plates $Y = 0$ and $Y = 1$, respectively. It is observed from these Figures that, increasing rarefaction as well as fluid wall interaction parameters yields an increase in the skin friction at $Y = 0$ while the reverse tread occurs at $Y = 1$. This effect is more significant as the wall-ambient temperature difference ratio decrease.

Figures $4.1.19 - 4.1.20$ and $4.1.21 - 4.1.22$ exhibit the combined effects of the Hall current parameter, rarefaction parameter as well as wall-ambient temperature difference ratio on the skin friction at the microchannel plates $Y = 0$

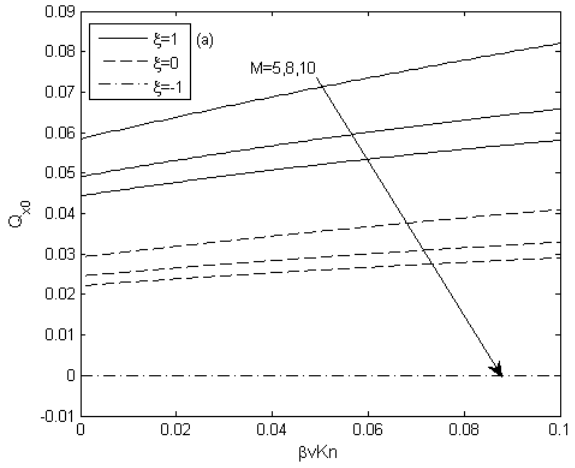


Figure 4.1.9: Volume flow rate versus $\beta_v Kn$ for different values of M due to primary flow when $In = 0.5$, $m = 0.5$

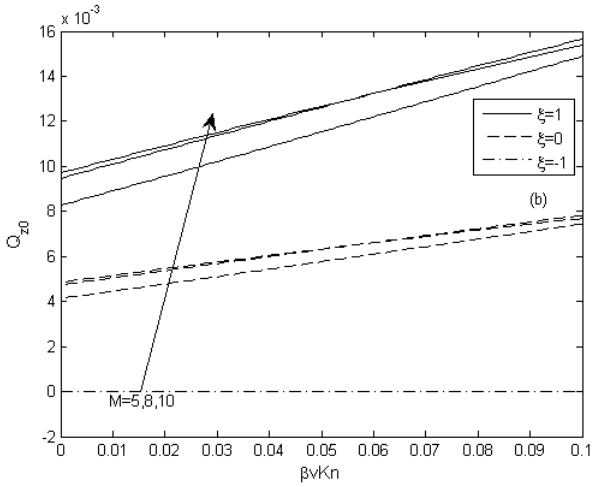


Figure 4.1.10: Volume flow rate versus $\beta_v Kn$ for different values of M due to secondary flow when $In = 0.5$, $m = 0.5$

and $Y = 1$, respectively. It is clearly seen that, increasing the value of Hall current parameter leads to enhancement in the skin friction in both cases at $Y = 0$ and $Y = 1$.

Figures 4.1.23 − 4.1.24 and 4.1.25 − 4.1.26 illustrate the combined effects of Hartmann number and rarefaction for different values of wall-ambient temperature difference ratio at the microchannel plates $Y = 0$ and $Y = 1$, respectively. It is evident that the skin-friction decreases with the increase in Hartmann number. In addition, the magnitude of skin-friction is higher in case of symmetric heating $\xi = 1$ in comparison with asymmetric heating of microchannel

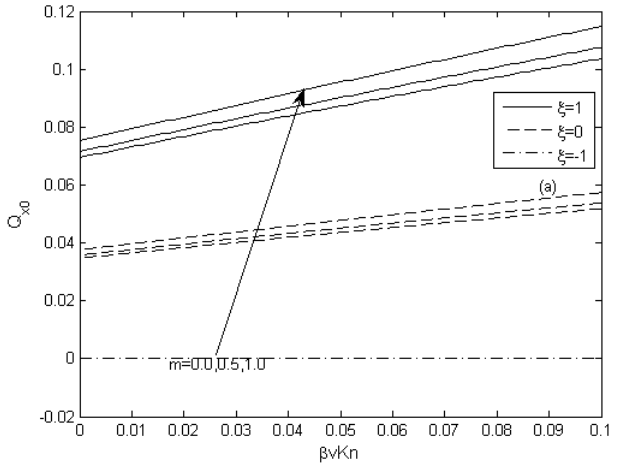


Figure 4.1.11: Volume flow rate versus $\beta_v Kn$ for different values of m due to primary flow when $M = 2$, $In = 1.667$

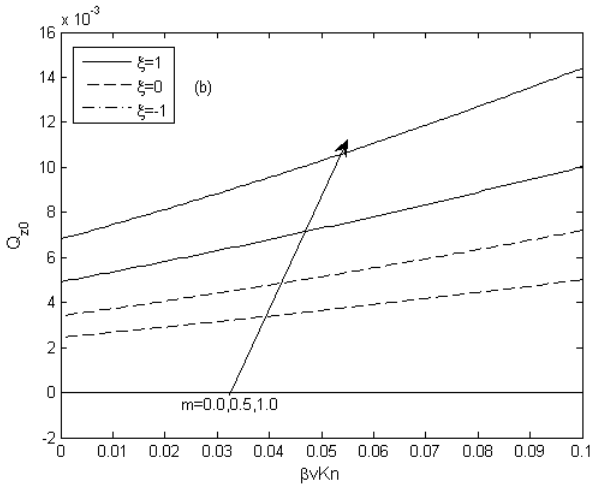


Figure 4.1.12: Volume flow rate versus $\beta_v Kn$ for different values of m due to secondary flow when $M = 2$, $In = 1.667$

plates $\xi = 0$.

Table 1 present numerical comparison of the present work for velocity with those of Chen and Weng (2005) when Hartmann number is neglected $M \longrightarrow 0$ and Jha et al.(2015) in the absence of Hall current ($m = 0$). This comparison gives an excellent agreement.

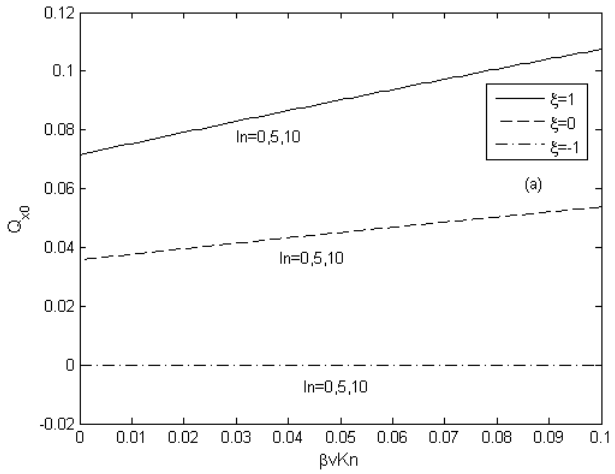


Figure 4.1.13: Volume flow rate versus $\beta_v Kn$ for different values of In due to primary flow when $M = 2$, $m = 0.5$

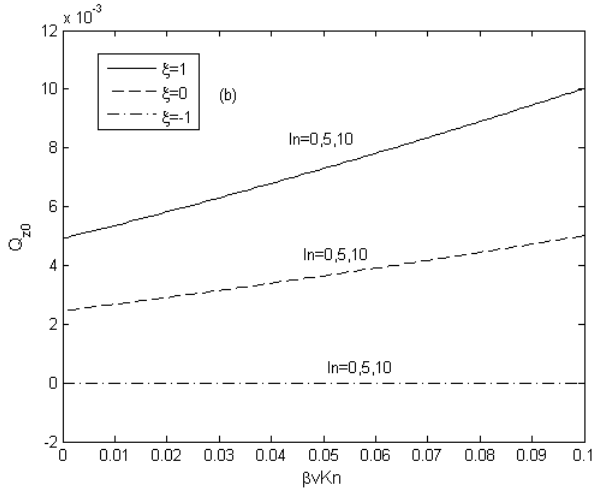


Figure 4.1.14: Volume flow rate versus $\beta_v Kn$ for different values of In due to secondary flow when $M = 2$, $m = 0.5$

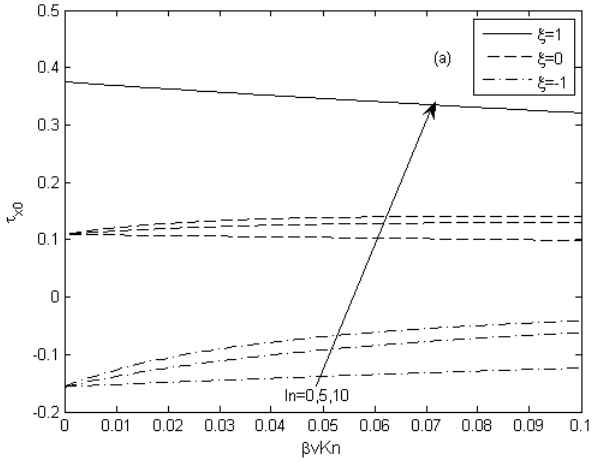


Figure 4.1.15: Variations of skin friction versus $\beta_v Kn$ for different values of In at $Y = 0$ due to primary flow when $M = 2$, $m = 0.5$

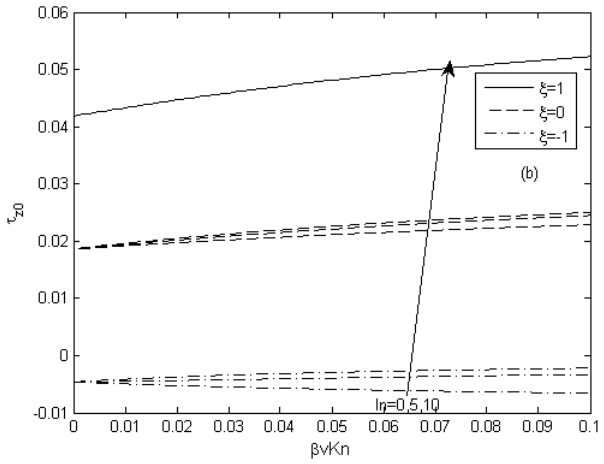


Figure 4.1.16: Variations of skin friction versus $\beta_v Kn$ for different values of In at $Y = 0$ due to secondary flow when $M = 2$, $m = 0.5$

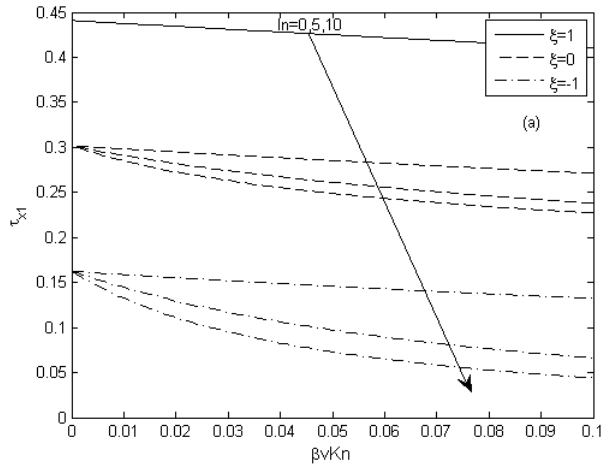


Figure 4.1.17: Variations of skin friction versus $\beta_v Kn$ for different values of In at $Y = 1$ due to primary flow when $M = 2$, $m = 0.5$

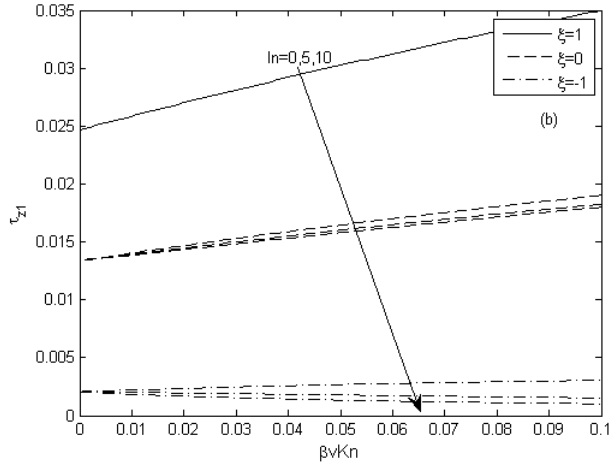


Figure 4.1.18: Variations of skin friction versus $\beta_v Kn$ for different values of In at $Y = 1$ due to secondary flow when $M = 2$, $m = 0.5$

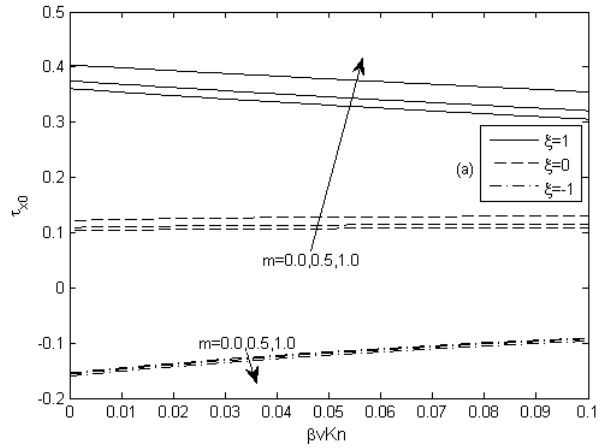


Figure 4.1.19: Variations of skin friction versus $\beta_v Kn$ for different values of m at $Y = 0$ due to primary flow when $M = 2$, $In = 1.667$

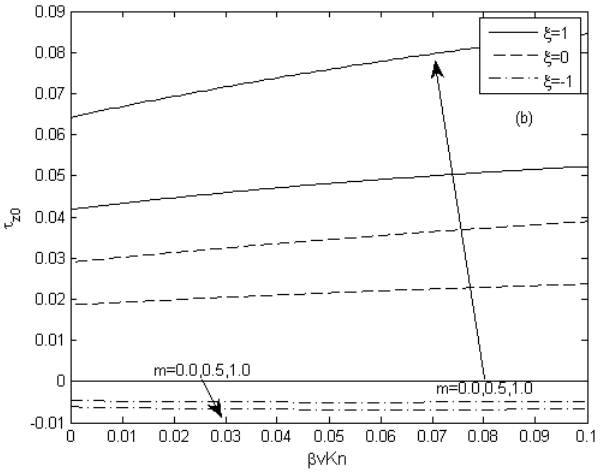


Figure 4.1.20: Variations of skin friction versus $\beta_v Kn$ for different values of m at $Y = 0$ due to secondary flow when $M = 2$, $In = 1.667$

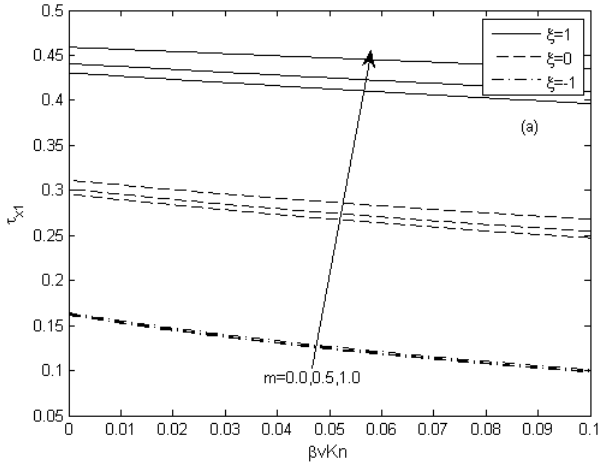


Figure 4.1.21: Variations of skin friction versus $\beta_v Kn$ for different values of m at $Y = 1$ due to primary flow when $M = 2$, $In = 1.667$

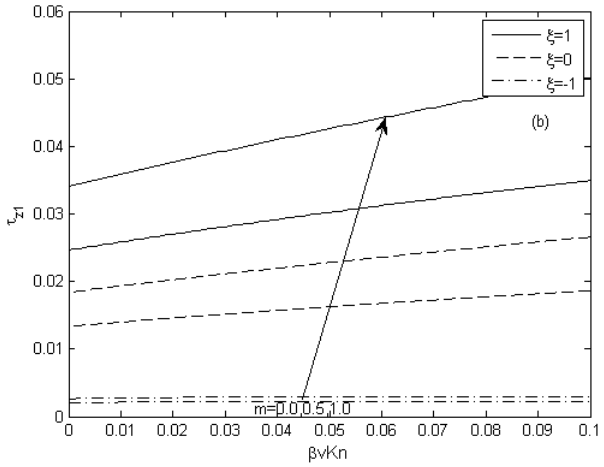


Figure 4.1.22: Variations of skin friction versus $\beta_v Kn$ for different values of m at $Y = 1$ due to secondary flow when $M = 2$, $In = 1.667$

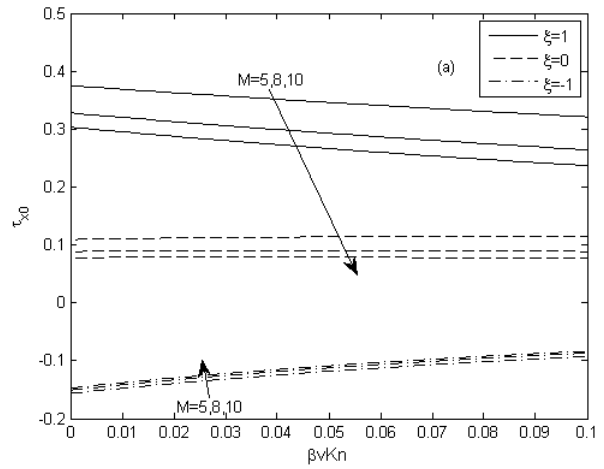


Figure 4.1.23: Variations of skin friction versus $\beta_v Kn$ for different values of M at $Y = 0$ due to primary flow when $m = 0.5$, $In = 1.667$

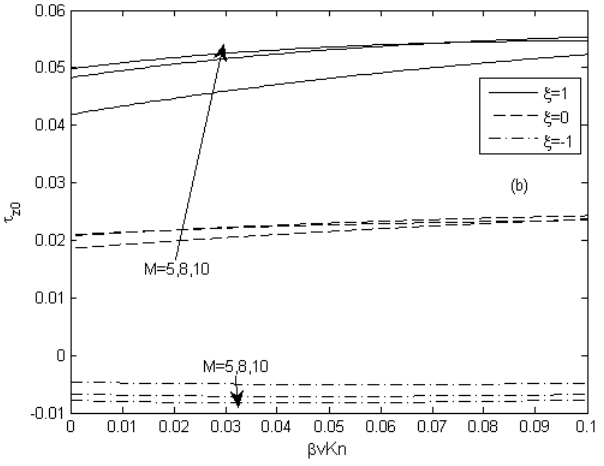


Figure 4.1.24: Variations of skin friction versus $\beta_v Kn$ for different values of M at $Y = 0$ due to secondary flow when $m = 0.5$, $In = 1.667$

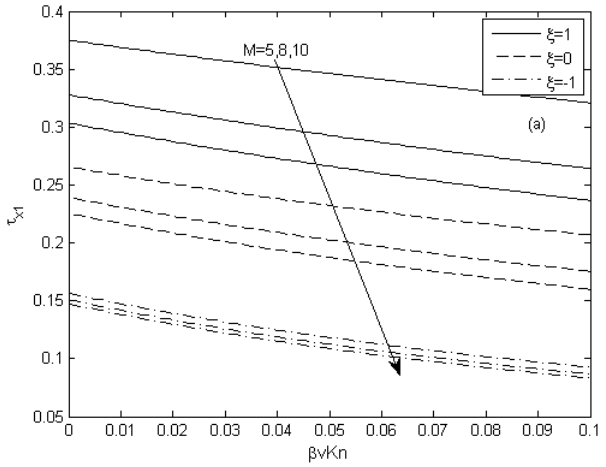


Figure 4.1.25: Variations of skin friction versus $\beta_v Kn$ for different values of M at $Y = 1$ due to primary flow when $m = 0.5$,$In = 1.667$

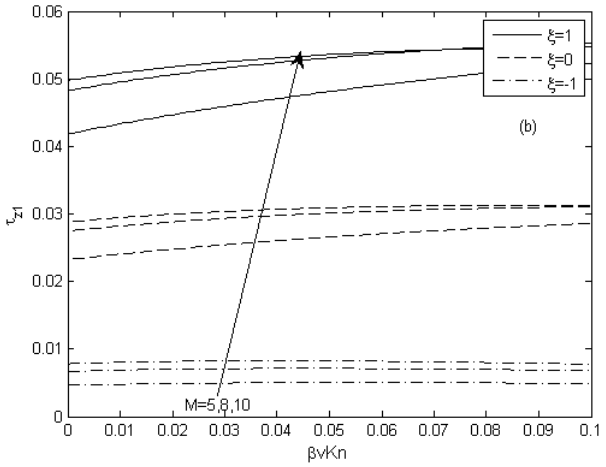


Figure 4.1.26: Variations of skin friction versus $\beta_v Kn$ for different values of M at $Y = 1$ due to secondary flow when $In = 1.667$, $m = 0.5$

Table 4.1: Numerical comparison of the values of the primary velocity (U) obtained in the present work with those of Chen and Weng (2005) and Jha *et al.* (2015)

velocity when $In = 1.667$, $\beta_v Kn = 0.05$					
ξ	Y	Chen and Weng	Present work	Jha *et al.*	Present work
		(2005)	(when M$\rightarrow$ 0)	(2015)	(when m=0)
1.0	0.2	0.1050	0.1050	0.0715	0.0715
	0.4	0.1450	0.1450	0.0694	0.0694
	0.6	0.1450	0.1450	0.0964	0.0964
	0.8	0.1050	0.1050	0.0715	0.0715
	1.0	0.0250	0.0250	0.0177	0.0177
0.0	0.2	0.0437	0.0437	0.0279	0.0279
	0.4	0.0684	0.0684	0.0446	0.0446
	0.6	0.0766	0.0766	0.0518	0.0518
	0.8	0.0613	0.0613	0.0436	0.0436
	1.0	0.0157	0.0157	0.0118	0.0118
-1.0	0.2	-0.0176	-0.0176	-0.0157	-0.0157
	0.4	-0.0082	-0.0082	-0.0072	-0.0072
	0.6	0.0081	0.0081	0.0072	0.0072
	0.8	0.0176	0.0176	0.0157	0.0157
	1.0	0.0065	0.0065	0.0059	0.0059

4.2 Fully developed MHD natural convection flow in a vertical micro-porous-channel with Hall effects

This section investigates the impact of suction/injection (S) on the microfluidic flow of a viscous incompressible and electrically conducting fluid subjected to an applied magnetic field in presence of Hall effect. Numerical values of governing parameters are arbitrarily taken as in case 1 above, whereas S is assumed to be 0.5 in the present problem.

Figures 4.2.1 – 4.2.2 shows the effect of the rarefaction parameter ($\beta_v Kn$) on primary and secondary velocity profiles. From the figures, it can be observed that as $\beta_v Kn$ increases, the velocity slip at the wall increases which reduces the retarding effect of the wall. This yields an observable increase in the fluid velocity near the wall. Further on, as the rarefaction parameter $\beta_v Kn$ and the wall ambient temperatures ξ increases, the amount of heat transfer from the wall to the fluid increase yielding an increase in buoyancy force which drives the flow and hence increasing the gas velocity in both primary and secondary directions.

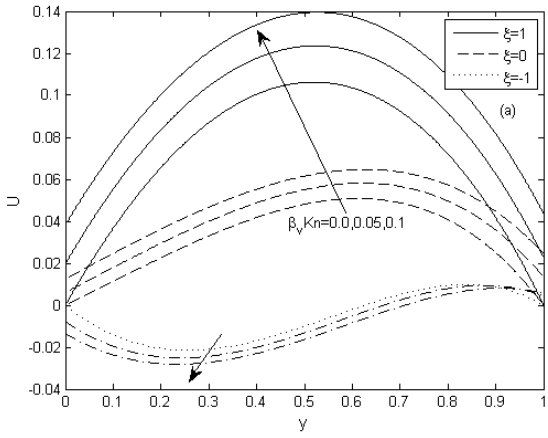


Figure 4.2.1: Primary velocity profiles for different values of $\beta_v Kn$ when $m = 0.5$, $S = 0.5$, $M = 2$ and $In = 1.667$

Figure 4.2.3 – 4.2.4 present the primary and secondary flow velocity for different values of the fluid wall interaction parameter (In). From the figures, it is

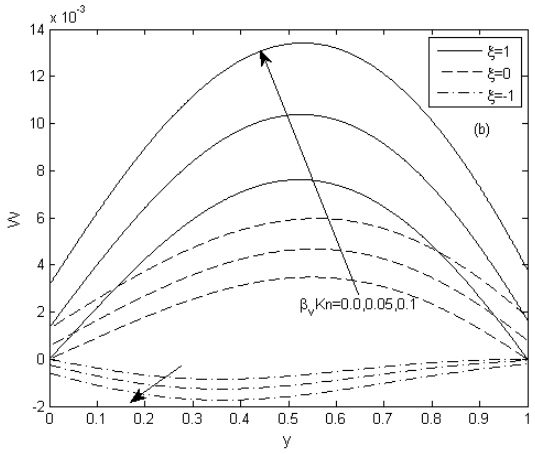


Figure 4.2.2: Secondary velocity profiles for different values of $\beta_v Kn$ when $m = 0.5$, $S = 0.5$, $M = 2$ and $In = 1.667$

clear that when the wall-ambient temperature difference ratio $\xi = 1$, increase in In has no significant effect on fluid velocity in both flow directions since the temperature of the fluid is not changing, while the effect becomes more pronounced as ξ decreases. It can also be observed that velocity slip increases on the microchannel surfaces with increase in In resulting to increase in fluid velocity. Fig. 4.2.(5-8) displays the effect of suction/injection on the primary and secondary velocity profiles. It can be observed that injection (positive value of S) causes an increase in the primary as well as secondary velocity profiles for all wall heating conditions ξ. Whereas suction (negative value of S) decreases it. This is attributed to the fact that for $S > 0$ cold fluid particles are injected into the micro-porous channel through the cold porous wall while fluid particles that are heated on the hot wall are removed out of the channel. This decreases the temperature in the channel thus weakening the convection current. This leads to a decrease in primary as well as secondary velocity profiles. Further on, it is evident that the effect of suction/injection parameter (S) on the micro-channel velocity slip and temperature jump becomes significant with the decrease of the wall - ambient temperature difference ratio ξ. The reverse phenomenon occurs when suction is applied on the cold porous wall with simultaneous injection on the hot porous wall ($S < 0$).

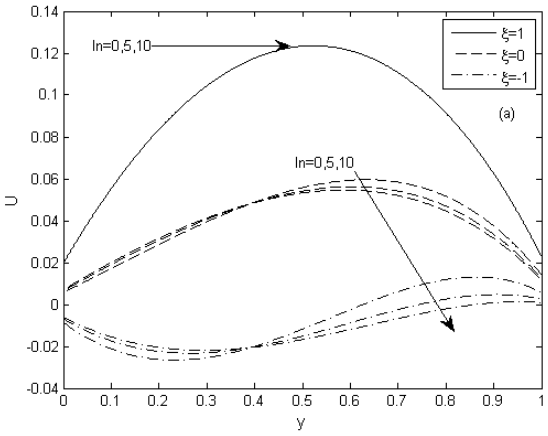


Figure 4.2.3: Primary velocity profiles for different values of In when $\beta_v Kn = 0.05$, $m = 0.5$, $S = 0.5$, $M = 2$

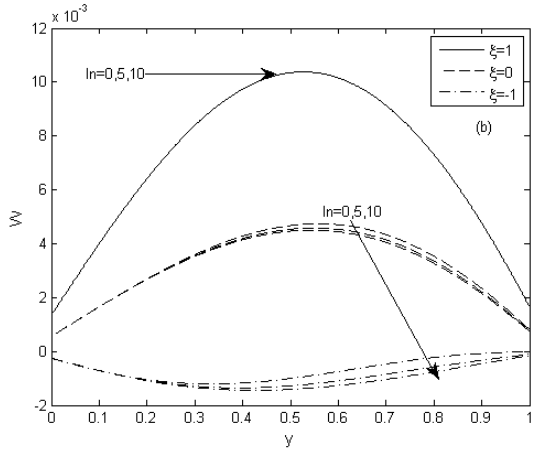


Figure 4.2.4: Secondary velocity profiles for different values of In when $\beta_v Kn = 0.05$, $m = 0.5$, $S = 0.5$, $M = 2$

Figures 4.2.9 and 4.2.10 shows the effect of the Hartmann number (M) on the fluid velocities. It is observed that the primary velocity decreases with increase in the magnetic field M while the secondary velocity increases with M. This can attributed to the classical Hartmann effect or the damping force induced by increasing the magnetic field on fluid velocity. Figure 4.2.11 and 4.2.12 reveals that the primary and secondary velocity increases with the Hall current parameter m for symmetric $\xi = 1$ and asymmetric $\xi = 0$ wall heating conditions. The Fig. also reveals that the fluid velocity increases steadily with increase in m along the primary direction while it overshoots along the secondary (W). This is physically true since U is the source of W, so increase

in the Hall currents reduces the magnetic damping force thereby increasing fluid velocity along the secondary flow direction.

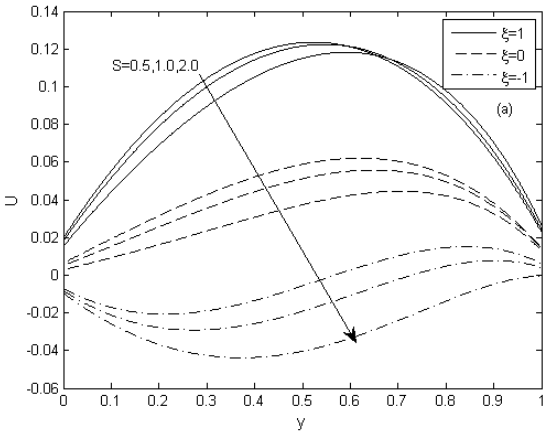


Figure 4.2.5: Primary velocity profiles for different values of Positive S (suction) when $\beta_v Kn = 0.05$, $m = 0.5$, $M = 2$, $In = 1.667$

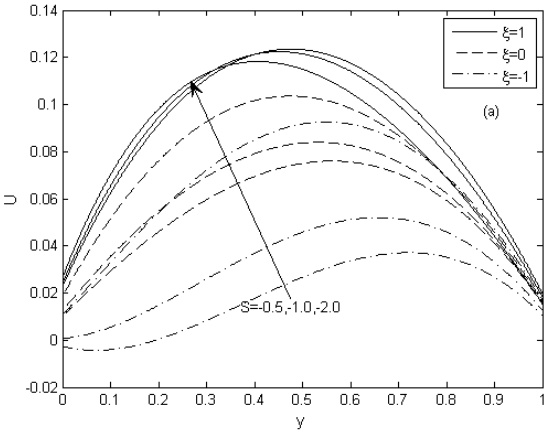


Figure 4.2.6: Primary velocity profiles for different values of negative S (injection) when $\beta_v Kn = 0.05$, $m = 0.5$, $M = 2$, $In = 1.667$

The effect of some governing parameters on the micro-fluidic volume flow (Q_{x0} (along the primary direction) and Q_{z0} (along the secondary direction)are presented in Figs. 4.2.13 - 4.2.20. From Figs. 4.2.(13-14), it was discovered that in both primary and transverse directions, the effect of the magnetic field M on the resultant volume flow is greatly influenced by the wall ambient temperatures ξ. This is because when $\xi = 1$, or 0 the volume flow in the flow directions decreases with the magnetic field, while it increases when $\xi = -1$. Increase in the rarefaction parameter $\beta_v Kn$ on the other hand, yields a decrease in the

volume flow for all values of ξ though not displayed.

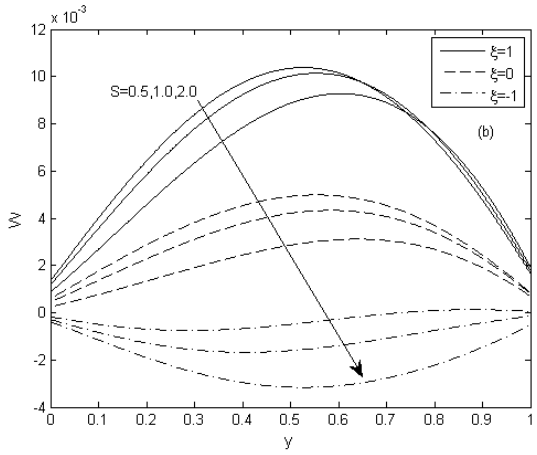


Figure 4.2.7: Secondary velocity profiles for different values of positive S (suction) when $\beta_v Kn = 0.05$, $m = 0.5$, $M = 2$, $In = 1.667$

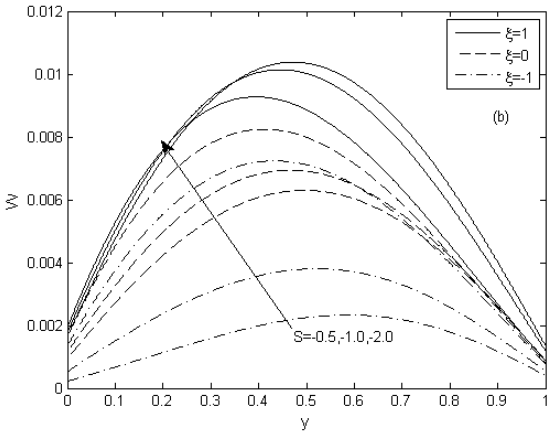


Figure 4.2.8: Secondary velocity profiles for different values of negative S (injection) when $\beta_v Kn = 0.05$, $m = 0.5$, $M = 2$, $In = 1.667$

Figure 4.2.(15-16) presents the effect of the Hall current parameter on volume flow in both primary and transverse flow directions. From the figures, it is evident that for symmetric and asymmetric heating ($\xi = 1, 0$) the resultant volume flow increases steadily in the flow direction while it overshoots in the transverse directions as m increases. It is also evident that Q_{x0} and Q_{z0} decreases with the Hall parameter when $\xi = -1$.This is physically true since increase in the Hall parameter reduces the effect of the magnetic field thereby enhancing the buoyancy force as observed in fig 4.2.9 and 4.2.10. From figures

4.2.17 and 4.2.18, it its noticed that for asymmetric heating, the volume flow increases with the fluid wall interaction parameter In when the rarefaction parameter $\beta_v Kn$ increases while the effect becomes insignificant when the two plates are heated symmetrically $\xi = 1$. It is also noticed that for small In, increase in $\beta_v Kn$ decreases the volume flow.

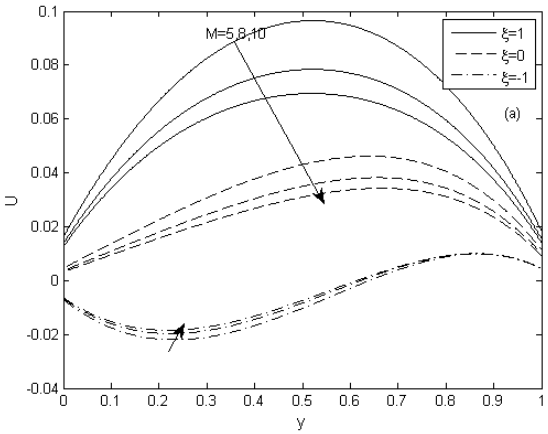


Figure 4.2.9: Primary velocity profiles for different values of M when $\beta_v Kn = 0.05$, $m = 0.5$, and $In = 1.667$ and $S = 0.5$

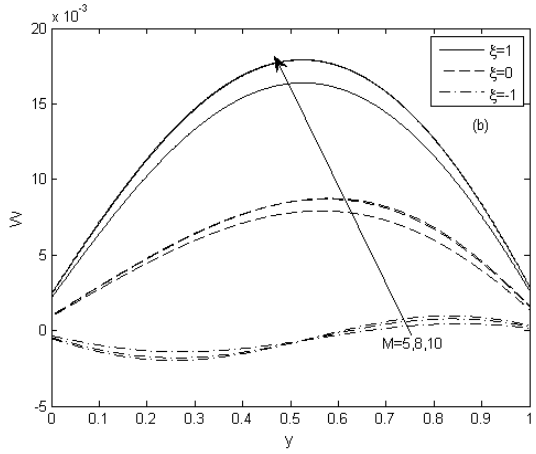


Figure 4.2.10: Secondary velocity profiles for different values of M when $\beta_v Kn = 0.05$, $m = 0.5$, $In = 1.667$ and $S = 0.5$

Figures 4.2.(17-18) presents the effect of the suction/injection parameter S on the microfluidic volume flow along the primary and transverse directions. As expected, we noticed that injection (negative value of S) has an increasing effect on the volume flow Q_{x0} and Q_{z0} while suction (positive value of S) has a decreasing effect as observed in 4.2.19 and 4.2.20. This can be traced to Fig.

4.2.(5-8), since the velocity increases with negative S while it decreases with positive S.

The wall skin friction (τ_x and τ_z) of the MHD natural convection in a vertical micro-channel in the presence of suction/injection are described in Figs. (4.2.21-4.2.36) at the walls $Y = 0$ and $Y = 1$. From Fig. 4.2.21 it is clear that τ_{x0} decreases with the magnetic field when $\xi = 1$ and $\xi = 0$. This is because increase in the magnetic field (M) creates a mechanical damping force which retards the fluid flow resulting to decrease in velocity in the primary direction of flow (Figs. 4.2.11-12) and subsequently the skin friction. In Fig. 4.2.22 however, the influence of the Hartmann (M) is completely opposite to that of Fig. 4.2.21 as τ_{x0} is seen to increase with M when $\xi = 1$ and $\xi = 0$. From the two figures, it is interesting to note that the rarefaction parameter has a negligible or no effect on the skin friction when $\xi = 0$. At the plate $Y = 1$ (Fig. 4.2.23-24), we see that τ_{x1} increases with the Harmann number while τ_{z1} decreases with increase in M.

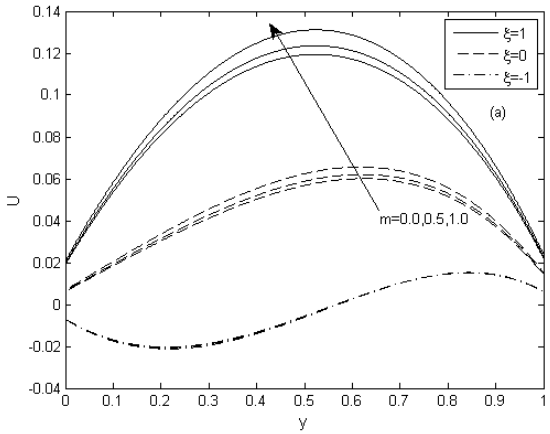


Figure 4.2.11: Primary velocity profiles for different values of m when $\beta_v Kn = 0.05$, $M = 2$, $In = 1.667$ and $S = 0.5$

Figures 4.2.25-4.2.28 shows the effect of the fluid wall interaction parameter (In) and the rarefaction parameter $\beta_v Kn$ on the skin friction on the boundary plates $Y = 0$ and the $Y = 1$ respectively. From Figures 4.2.25 and 4.2.26 at $Y = 0$ we observe that τ_{x0} and τ_{z0} simultaneously increases with the fluid wall interaction parameter In but the increase is more evident for asymmetric heat-

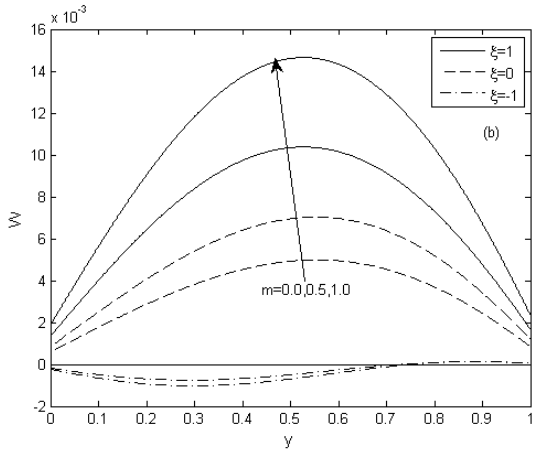


Figure 4.2.12: Secondary velocity profiles for different values of m when $\beta_v Kn = 0.05$, $M = 2$ and $S = 0.5$ and $In = 1.667$

ing ($\xi = 0, -1$). For symmetric heating however, increase in $\beta_v Kn$ decreases the skin friction τ_{x0} and τ_{z0}. It was observed that the contribution of the wall ambient temperatures ξ to the resultant skin friction is strongly dependent on the value of the rarefaction parameter $\beta_v Kn$. At the plate $Y = 1$ Figs 4.2.27 and 4.2.28, the influence of the fluid wall interaction parameter is observe to increase the skin friction.

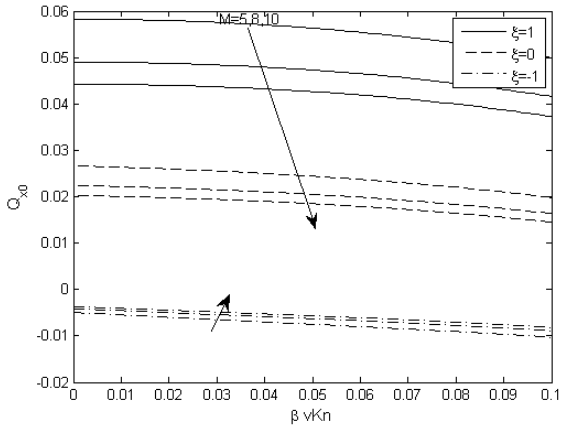


Figure 4.2.13: Volume flow rate versus $\beta_v Kn$ for different values of M when $m = 0.5$, $S = 0.5$ and $In = 1.667$ due to primary flow

The effects of Hall parameter and rarefaction parameter on the primary and secondary skin friction on the plates $Y = 0$ and $Y = 1$ are depicted in Fig. 4.2.(29-32) respectively. From the figures, we observed the primary and secondary skin friction increases with the Hall parameter m at the left plate

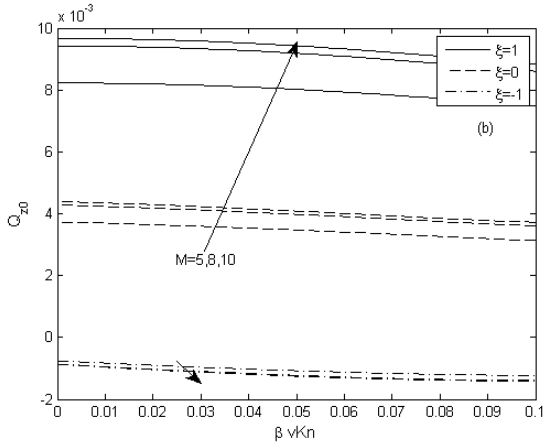


Figure 4.2.14: Volume flow rate versus $\beta_v Kn$ for different values of M when $m = 0.5$, $S = 0.5$ and $In = 1.667$ due to secondary flow

$Y = 0$ while it decreases at the upper plate $Y = 1$. In Figures 4.2.(33-36), the skin friction at the primary and transverse direction for variations in the suction/injection parameter S are shown. It is found from the two figures that suction decreases the resultant skin friction while it increases with injection. It can also be observed that for asymmetric heating ($\xi = -1$), the resultant skin friction overshoots with negative values of S.

Table 2 present numerical comparison of the present work for velocity with Jha et al.(2015b) in the absence of Hall current ($m = 0$). This comparison gives an excellent agreement.

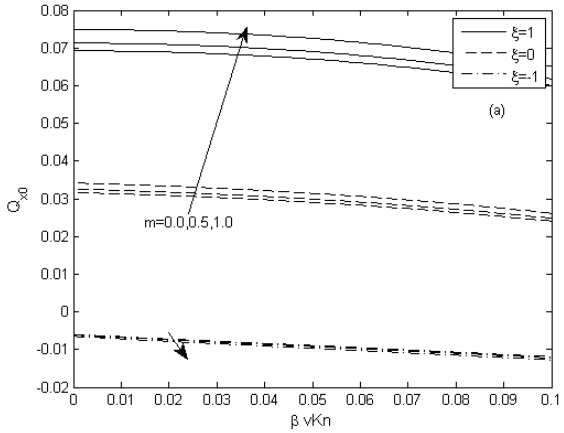


Figure 4.2.15: Volume flow rate versus $\beta_v Kn$ for different values of m when $M = 2$, $S = 0.5$ and $In = 1.667$ due to primary flow

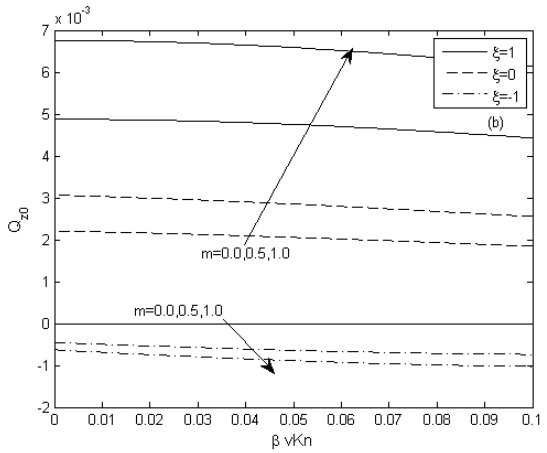


Figure 4.2.16: Volume flow rate versus $\beta_v Kn$ for different values of m when $M = 2$, $S = 0.5$ and $In = 1.667$ due to secondary flow

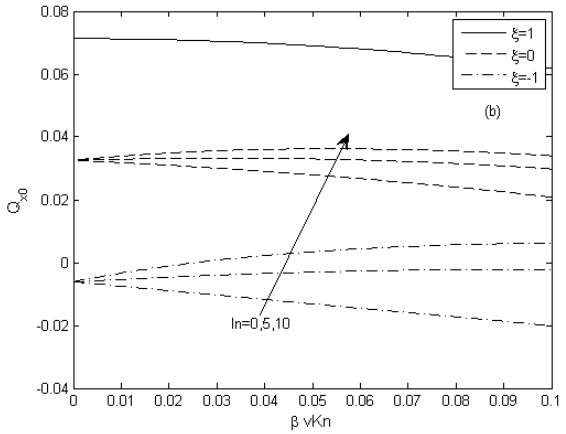


Figure 4.2.17: Volume flow rate versus $\beta_v Kn$ for different values of In when $M = 2$, $S = 0.5$ and $m = 0.5$ due to primary flow

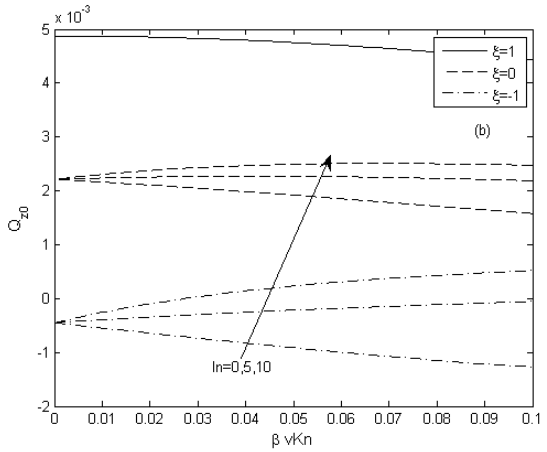


Figure 4.2.18: Volume flow rate versus $\beta_v Kn$ for different values of In when $M = 2$, $S = 0.5$ and $m = 0.5$ due to secondary flow

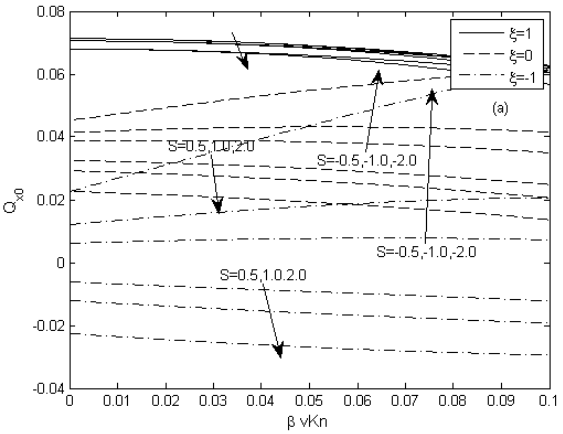


Figure 4.2.19: Volume flow rate versus $\beta_v Kn$ for different values of S when $M = 2$, $In = 1.667$ and $m = 0.5$ due to primary flow

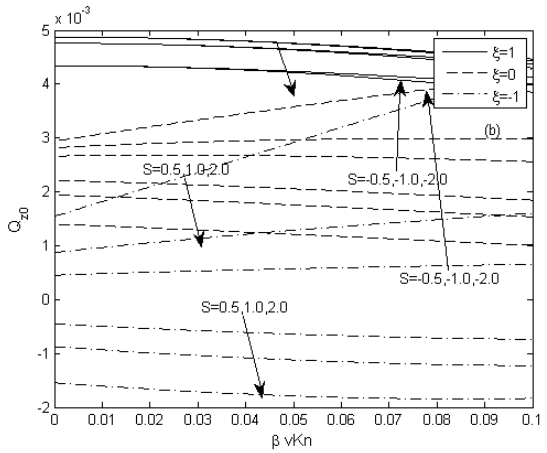


Figure 4.2.20: Volume flow rate versus $\beta_v Kn$ for different values of S when $M = 2$, $In = 1.667$ and $m = 0.5$ due to secondary flow

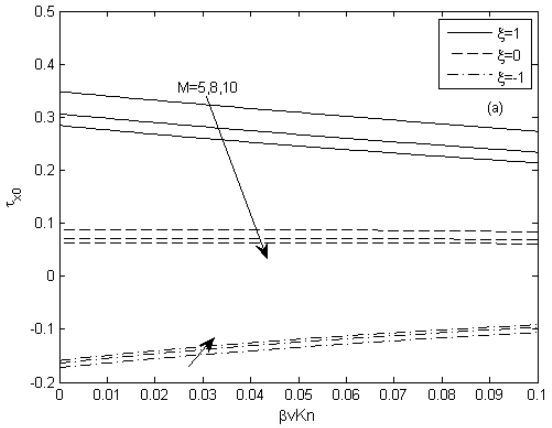


Figure 4.2.21: Variations of skin friction versus $\beta_v Kn$ for different values of M at $Y = 0$ due to primary flow when $In = 1.667$, $m = 0.5$,$S = 0.5$

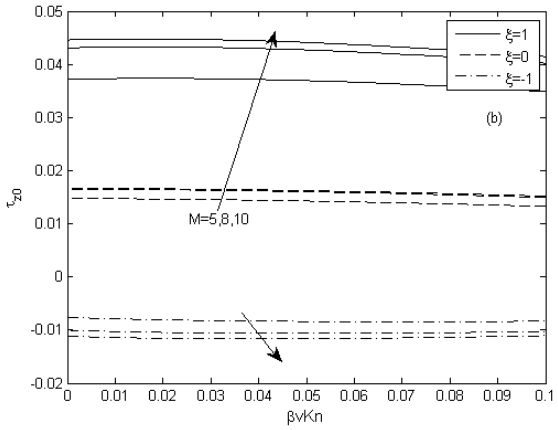


Figure 4.2.22: Variations of skin friction versus $\beta_v Kn$ for different values of M at $Y = 0$ due to secondary flow when $In = 1.667$, $m = 0.5$,$S = 0.5$

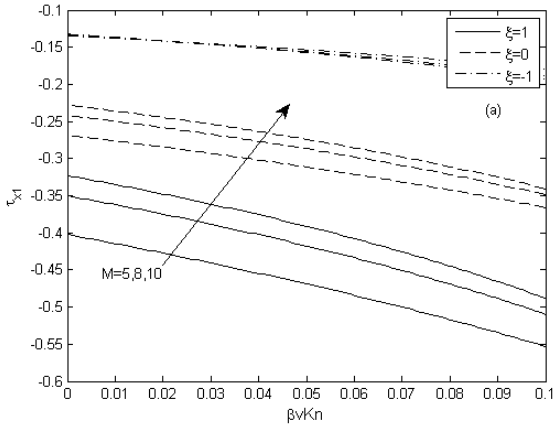


Figure 4.2.23: Variations of skin friction versus $\beta_v Kn$ for different values of M at $Y = 1$ due to primary flow when $In = 1.667$, $m = 0.5$,$S = 0.5$

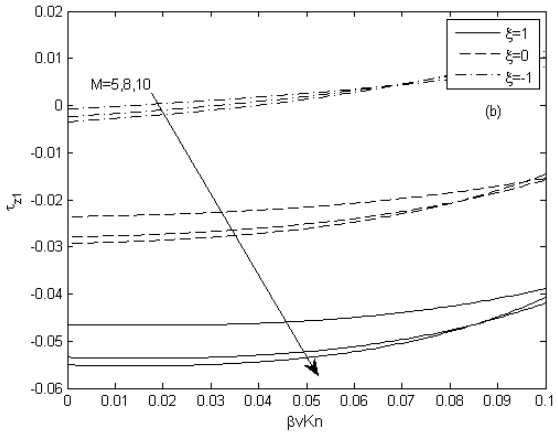


Figure 4.2.24: Variations of skin friction versus $\beta_v Kn$ for different values of M at $Y = 1$ due to secondary flow when $In = 1.667$, $m = 0.5$,$S = 0.5$

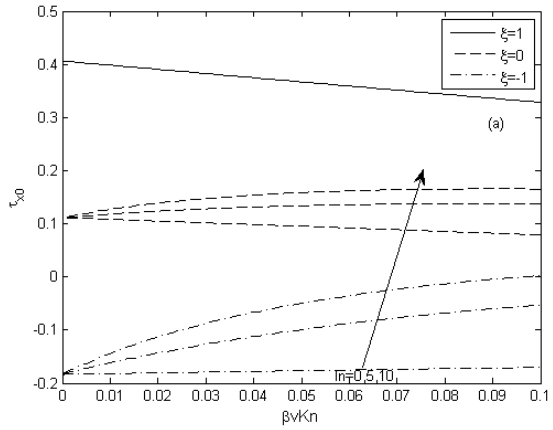


Figure 4.2.25: Variations of skin friction versus $\beta_v Kn$ for different values of In at $Y = 0$ due to primary flow when $M = 2$, $m = 0.5$,$S = 0.5$

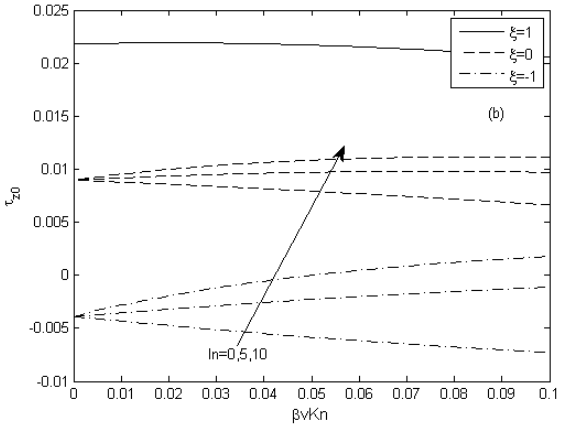


Figure 4.2.26: Variations of skin friction versus $\beta_v Kn$ for different values of In at $Y = 0$ due to secondary flow when $M = 2$, $m = 0.5$,$S = 0.5$

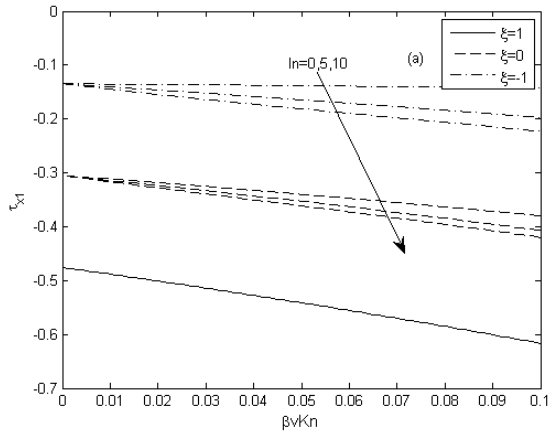


Figure 4.2.27: Variations of skin friction versus $\beta_v Kn$ for different values of In at $Y = 1$ due to primary flow when $M = 2$, $m = 0.5$,$S = 0.5$

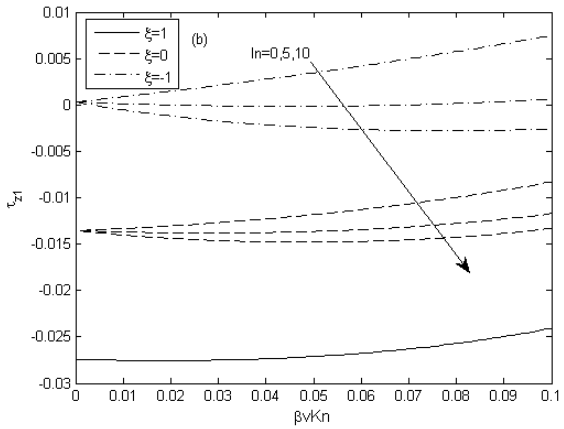


Figure 4.2.28: Variations of skin friction versus $\beta_v Kn$ for different values of In at $Y = 1$ due to secondary flow when $M = 2$, $m = 0.5$, $S = 0.5$

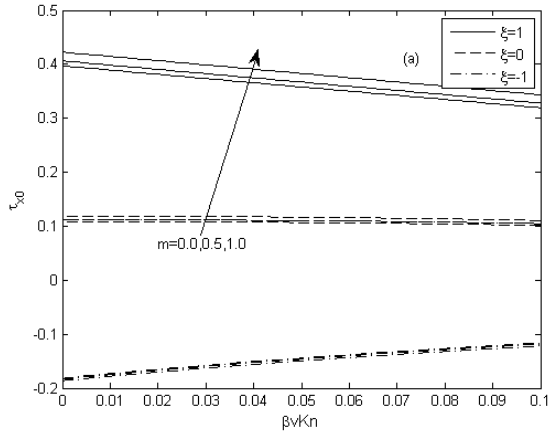


Figure 4.2.29: Variations of skin friction versus $\beta_v Kn$ for different values of m at $Y = 0$ due to primary flow when $M = 2$, $In = 1.667$, $S = 0.5$

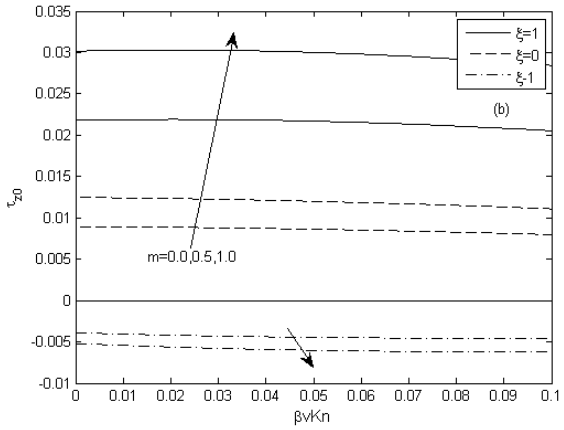


Figure 4.2.30: Variations of skin friction versus $\beta_v Kn$ for different values of m at $Y = 0$ due to secondary flow when $M = 2$, $In = 1.667$, $S = 0.5$

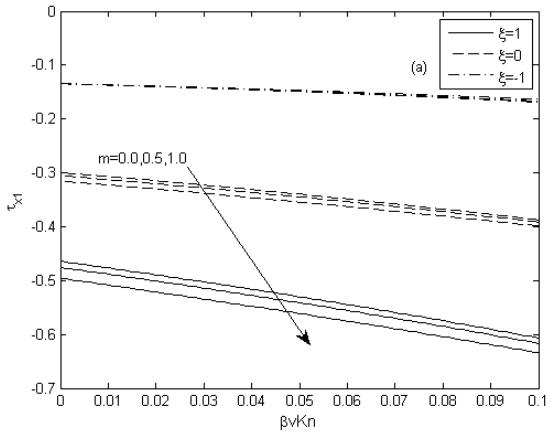


Figure 4.2.31: Variations of skin friction versus $\beta_v Kn$ for different values of m at $Y = 1$ due to primary flow when $M = 2$, $In = 1.667$,$S = 0.5$

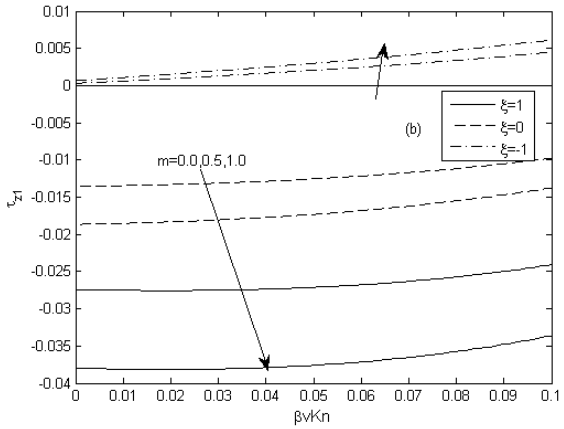


Figure 4.2.32: Variations of skin friction versus $\beta_v Kn$ for different values of m at $Y = 1$ due to secondary flow when $M = 2$, $In = 1.667$, $S = 0.5$

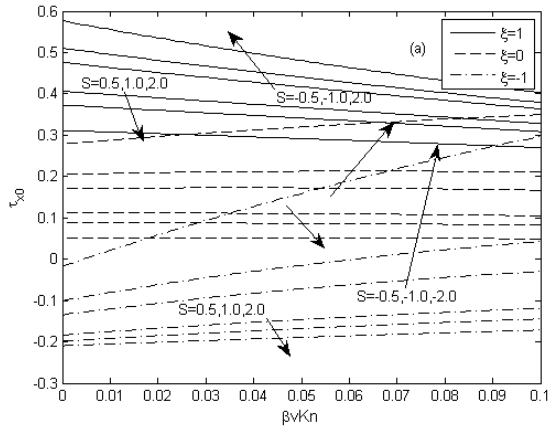


Figure 4.2.33: Variations of skin friction versus $\beta_v Kn$ for different values of S at $Y = 0$ due to primary flow when $M = 2$, $In = 1.667$, $m = 0.5$

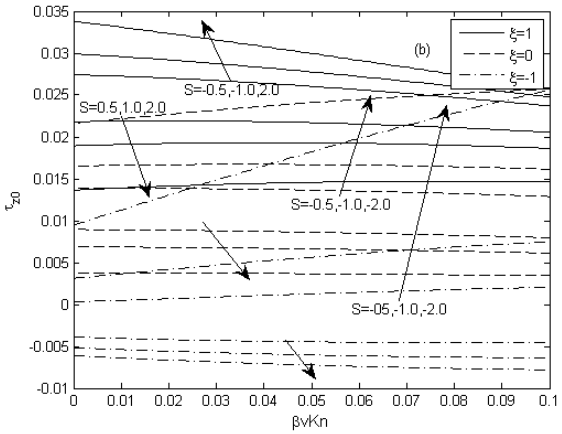


Figure 4.2.34: Variations of skin friction versus $\beta_v Kn$ for different values of S at $Y = 0$ due to secondary flow when $M = 2$, $In = 1.667$, $m = 0.5$

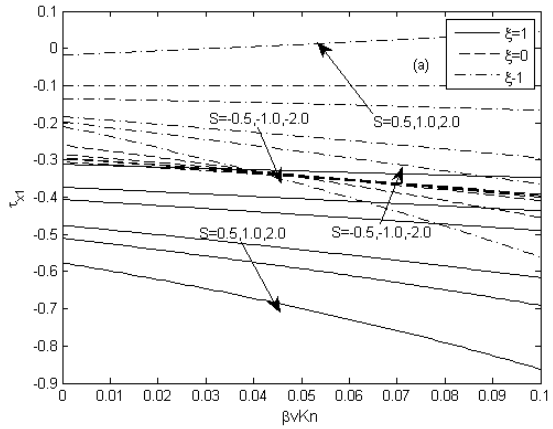


Figure 4.2.35: Variations of skin friction versus $\beta_v Kn$ for different values of S at $Y = 1$ due to primary flow when $M = 2$, $In = 1.667$, $m = 0.5$

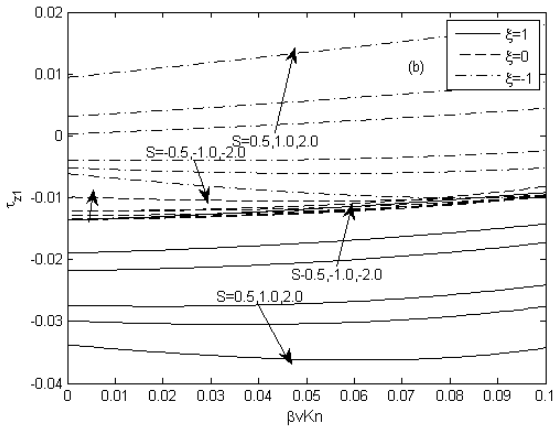


Figure 4.2.36: Variations of skin friction versus $\beta_v Kn$ for different values of S at $Y = 1$ due to secondary flow when $M = 2$, $In = 1.667$, $m = 0.5$

Table 4.2: Numerical comparison of the values of the primary velocity (U) obtained in the present work with Jha *et al.* (2015b)

velocity when $In = 1.667$,$S = 0.5$, $M = 2$ $\beta_v Kn = 0.05$			
ξ	Y	Jha *et al.*	Present work
		(2015)	(when m=0)
1.0	0.2	0.0809	0.0809
	0.4	0.1137	0.1137
	0.6	0.1171	0.1171
	0.8	0.0885	0.0885
	1.0	0.0221	0.0221
0.0	0.2	0.0284	0.0284
	0.4	0.0470	0.0470
	0.6	0.0561	0.0561
	0.8	0.0483	0.0483
	1.0	0.0132	0.0132
-1.0	0.2	-0.0241	-0.0241
	0.4	-0.0196	-0.0196
	0.6	-0.0049	-0.0049
	0.8	0.0080	0.0080
	1.0	0.0044	0.0044

CHAPTER FIVE

SUMMARY, CONCLUSION AND RECOMMENDATION

5.1 Summary

This dissertation presents a study on buoyancy driven flow of conducting fluid in a vertical micro-channel with Hall effect. Two models are presented, the first investigates Hall effect on MHD natural convection flow in a vertical micro-channel while the second problem examines fully developed MHD Natural Convection flow in a vertical Micro-Porous-Channel with Hall effect. In both cases, the micro-channel surfaces are either heated asymmetrically or symmetrically as dictated by the wall-ambient temperature difference ratio, due to influence of the transversely applied magnetic field on conducting fluid, a current is produced in a direction perpendicular to both electric and magnetic forces, as a result, the electrical conductivity becomes anisotropic and this generates secondary flow in the transverse direction. The governing momentum and energy equations subject to relevant boundary conditions are obtained and presented in dimensional form under the Boussinesq approximation. Using some non-dimensional parameters, the governing equations are reduced to dimensionless form and exact solution is obtained analytically by employing the method of undetermined coefficient. The effects of the various governing parameters on primary and secondary velocity, volume flow rates and skin friction are analysed and discussed.

5.2 Conclusion

Using the MATLAB software package, hydrodynamic response of the fluid flow to various flow parameters like Hartmann number (Ha), Hall current parameter (m), rarefaction parameter ($\beta_v Kn$), fluid interaction parameter (In), suction/injection (S) and wall-ambient temperature difference ratio (ξ) are presented graphically to have a physical insight into the problem. The problem was validated numerically, an excellent agreement is found with Jha *et al* (2015) in the absence of Hall current and also the work of Chen and Weng (2005) when the Hartmann number is negligibly small as displayed in table 1. The main conclusions of the present study are: For

Hall Effect on MHD natural convection flow in a vertical microchannel

1. The impact of the fluid wall interaction is found to enhance both primary and secondary velocity profiles.

2. Increasing the wall ambient temperature difference ratio and rarefaction parameter leads to enhancement in fluid velocity and velocity slip in both primary and secondary flow directions.

3. It is found that, increase in Hall current parameter leads to increase in resultant velocity (primary and secondary) and skin friction due to primary and secondary flow.

4. Hartmann number has a strong influence on flow formation in both primary and secondary flow directions.

Fully developed MHD natural convection flow in a vertical microporous-channel with Hall effects

5. Increase in $\beta_v Kn$ increases the slip due to rarefaction and reduces the

fluid-plate molecular interactions thereby decreasing the velocity near the cold wall.

6. It is observed that velocity decreases with increase in S (injection) and increases with decrease in S (suction) in both primary and secondary flow directions.

7. It is observed that the primary velocity decreases with increase in M while the secondary velocity increases with M.

8. The effect of the Hall current parameter on the volume flow in both the primary and the transverse flow directions is dependent on the wall ambient difference ratio (ξ). It is evident that for symmetric and asymmetric heating ($\xi = 1, 0$) the resultant volume flow increases steadily in the flow direction while it overshoots in the transverse directions as m increases.

5.3 Recommendation

The present study on buoyancy driven flow of conducting fluid in a vertical micro-channel with Hall effect is applicable in many devices at the microlevel like micro-pump, micro-heat exchangers, Hall actuators, Hall transducers, micro-sensors, micro-mixers, computer microchips, Microelectromechanical system (MEMS) e.t.c. as required for technological demanded. Also, the results obtained will not only provide useful information for industrial or engineering applications but also serve as an improvement on the previous studies related to such flows. This research could be extended to capture the influence of the induced magnetic fields and ion-slip current.

REFERENCES

Abo-El-Dahab, E.M.H. (1993) Effect of Hall currents on some magneto-hydrodynamic flow problems. *Master Thesis, Department of Mathematics, Faculty of Science, Helwan University, Egypt.*55-70

Attia, H.A. (2008) Effect of Hall current on transient hydromagnetic Couette-Poiseuille flow of a viscoelastic fluid with heat transfer. *Appl. Math. Modelling*, 32(4):375-388.

Avci, M. & Aydin, O. (2009) Mixed convection in a vertical microannulus between two concentric microtubes, *J. Heat Transfer Trans. ASME*, 131(7): 014502

Avci, M. & Aydin O. (2007) Mixed convection in a vertical parallel plate microchannel, *J. Heat Transfer Trans. ASME*, 129(12): 162-166.

Ali, A. O, Makinde, O. D. & Nkansah-Gyekye, Y. (2015) Effect of Hall Current on Unsteady MHD Couette Flow and Heat Transfer of Nano fluids in a Rotating System. *Applied and Computational Mathematics*, 4(9):232-244.

Buonomo, B. & Manca, O. (2012) Natural Convection Flow in a Vertical Micro-Channel with Heated at Uniform Heat Flux. *Int. J. Therm. Sci.*, 49(4): 1333-1344

Buonomo, B. & Manca, O. (2012) Transient Natural Convection Flow in a Vertical Micro-Channel with Heated at Uniform Heat Flux. *Int. J. Therm. Sci*, 56(2): 35-47

Cowling, T. G. (1957). Magnetohydrodynamics, *Interscience Pub., New York.*120-129.

Chen, C. K & Weng H.C. (2005) Natural convection in a vertical microchannel. *J Heat Transfer* , 127(12): 1053-6.

Eckert, E .R. G., & Drake, R. M., (1972) *Jr. Analysis of Heat and Mass Transfer*, *Mcgraw-Hill, New York*, 1102-1150.

Goniak, R. & Duffa, G. (1995) "Corrective Term in Wall Slip Equations for Knudsen Layer" *J. Thermophys. Heat Transfer,* 9(2): 383-384.

Ghosh S.K., & Bhattacharjee P.K. (2000) Magnetohydrodynamic convection flow in a rotating channel. *Arch. Mech*, 52(15):303-318.

Jha, B. K. Aina, B. & Joseph. S. B. (2014) Natural Convection Flow in vertical Micro-channel with Suction/Injection, *Journal of Process Mechanical Engineering*, 228 (3): 171-180

Jha, B. K. & Aina, B. (2014) Mathematical modelling and exact solution of steady fully developed mixed convection flow in a vertical microporous-annulus, Journal of *Afrika Matematika*,10(4):014-0277

Jha, B. K, Aina, B. & Ajiya, A. T. (2015) MHD Natural convection in a vertical parallel plate microchannel.*Ain Sham Eng. Journal*, 6:289-295.

Jha, B. K., Aina, B. & Ajiya, A. T. (2015b) Role of Suction/Injection on MHD Natural Convection Flow in a Vertical Microchannel, *International Journal of Energy and Technology*, 7(12):30-39.

Jha, B. K., Babatunde, A. & Sani, I. (2015) Transient Magnetohydrodynamic Free Convective Flow in Vertical Micro-Concentric-Annuli, *Process Mech. E. Part N: J Nanoengineering and Nanosystems*, 10(6):1177-1190.

Jha, B. K., Babatunde, A. & Sani, I, (2015) Fully Developed MHD Natural Convection Flow in a Vertical Annular Microchannel: An exact

solution, *Journal of King Saud university- Science*, 27: 253-259

Jha, B. K. & Aina, B., (2016) MHD Natural Convection flow in a Vertical Micro-Porous- Annulus in the Presence of Radial Magnetic Field, *Journal of Nanofluids*, 5(6): 292-301

Jha, B. K, Babatunde, A. & Sani, I, (2016) MHD Natural Convection flow in a Vertical Micro-Concentric-Annuli in the Presence of Radial Magnetic Field: An Exact Solution, Journal of *Ain Shams Engineering Journal*, 7(2):1061-1068

Jha, B.K. & Apere, Clement A. (2010) Combined effect of Hall and ion-slip currents on unsteady MHD Couette flow in a rotation system. *Journal of the Phys. Society of Japan* 79,104401. doi: 10(9):1143-1150.

Jha, B.K. & Apere, Clement A. (2011) Hall and ion-slip effect on unsteady MHD Couette flow in a rotation system with suction and injection. *Journal of the Phys. Society of Japan* 80:114401. doi: 10(80):1143.

Khadrawi, A. & Al-Nimr, M. A. (2007) Unsteady natural convection fluid flow in a vertical microchannel under the effect of the Dual-Phase-Lag heat conduction model, *International J. Thermophysics*, 28(4): 1387-1400.

Ram, P. C. (1995) Effects of Hall and ion-slip currents on free convective heat generating flow in a rotating fluid. *Int. J. Energy Res*, 19(4):371.

Seth, G.S. Sarkar, S. and Hussain, S. M. (2014). Effects of Hall current, radiation and rotation on natural convection heat and mass transfer flow past a moving vertical plate, *Ain Shams Engineering Journal*, 5 (2): 489-503.

Seth, G. S. Singh, J. K. & Mahato, G. K. (2012) Effects of Hall current

and rotation on unsteady hydromagnetic Couette flow within a porous channel, *International Journal of Applied Mechanics*, 4 (02): 1250015.

Seth, G. S., Nandkeolyar, R. & Ansari, Md.S. (2015) Effects of Hall Current and Rotation on Unsteady MHD Couette Flow in the Presence of an Inclined Magnetic Field, *Journal of Applied Fluid Mechanics*, 8 (1):7-20.

Singh, A. K. (1984) Hall effect on MHD Free-convection flow past an accelerated vertical porous plate. Reidel Publishing Company. *Astrophysics and space science*, 102:213-221.

Schaaf, S. A.& Chambre, P. L. (1961) Flow of Rarefied Gases, *Princeton University Press, Princeton.* pp. 55-70.

Seth, G.S., Sarkar S. & Makinde, O.D. (2016) Combined free and forced convection Couette-Harmann flow in rotating channel with arbitrary conducting walls and Hall effects, *Journal of Mechanics*, 32 (5): 613-629.

Seth, G.S. & Ansari Md. S., (2009) magnetohydrodynamic convective flow in a rotating channel with Hall effects, *International Journal of Theoretical and Applied Mechanics*, 4 (2):205-222

Sutton, G. & Sherman, A., (1965) Engineering Magnetohydrodynamics (*McGraw-Hill, New York*) pp. 150-312.

Seth, G.S. & Singh, J.K. (2015) Mixed convection hydromagnetic flow in a rotating channel with Hall and wall conductance effects. J. *of Appl. Math. Modelling. Elsevier.*,40(12):2783-2803.

APPENDIX A: Hall Effect on MHD natural convection flow in a vertical micro-channel.(1^{st} Case)

$A_0 = \xi + \frac{\beta_v Kn(1-\xi)}{1+2\beta_v Knln}$

$A_1 = \frac{1-\xi}{1+2\beta_v Knln}$

$a_1 = \beta_v KnM_1$

$a_2 = \frac{1}{M_1^2(A_1\beta_v Kn - A_0)}$

$a_3 = cosh(M_1) + M_1\beta_v Knsinh(M_1)$

$a_4 = sinh(M_1) + M_1\beta_v Kncosh(M_1)$

$a_5 = \frac{(A_0+A_1)+A_1\beta_v Kn}{M_1^2}$

$C_1 = \frac{a_1a_5+a_2a_4}{a_4+a_1a_3}$

$C_2 = \frac{a_5-a_2a_3}{a_4+a_1a_3}$

APPENDIX B: Fully developed MHD natural convection flow in a vertical micro-porous-channel with Hall effects (2^{nd} case)

$h_1 = 1 - \beta_v KnInSPr$

$h_2 = exp(SPr) + \beta_v KnInSPrexp(SPr)$

$A = \frac{\xi h_2 - h_1}{h_2 - h_1}$

$B = \frac{\xi - 1}{h_1 - h_2}$

$B_0 = \frac{B}{M_1^2 - S^2Pr^2 - S^2Pr}$

$C_2 = \frac{K_6K_7 - K_9K_4}{K_5K_7 - K_8K_4}$

$C_1 = \frac{K_6K_8 - K_9K_5}{K_4K_8 - K_7K_5}$

$b_1 = S/2$

$b_2 = S^2/4 + M_1^2$

$K_1 = b_1 + \sqrt{b_2}$

$K_2 = b_1 - \sqrt{b_2}$

$K_3 = \frac{B}{S^2Pr^2 - S^2Pr - M_1^2}$

$K_4 = 1 - \beta_v KnK_1 \; K_5 = 1 - \beta_v KnK_2 \; K_6 = K_3 - \frac{A}{M_1^2} - \beta_v KnK_3SPr$

$K_7 = exp(K_1) + \beta_v KnK_1exp(K_1)$

$K_8 = exp(K_2) + \beta_v KnK_2exp(K_2)$

$K_9 = K_3exp(SPr) - \frac{A}{M_1^2} - \beta_v KnK_3SPrexp(SPr)$

MATLAB PROGRAMS

```
%Hall effect on MHD natural convection flow in a vertical microchannel
clc
h=0.001;
%y=0;
[y]=0:h:1;
m=0.5;
%BvKn=0:h:0.1;
BvKn=0.05;
ln=1.667;
zi=1;
I=sqrt(-1);
M2=2;
M12=M2./(1+I.*m);
M1=sqrt(M12);
Ao=zi+(BvKn.*ln.*(1-zi))./(1+2.*BvKn.*ln);
A1=(1-zi)./(1+2.*BvKn.*ln);
a1=BvKn.*M1;
a2=(1./M12).*(A1.*BvKn-Ao);
a3=cosh(M1)+M1.*BvKn.*sinh(M1);
a4=sinh(M1)+M1.*BvKn.*cosh(M1);
a5=-((Ao+A1)+A1.*BvKn)./M12;
C2=(a5-a2.*a3)./(a4+a1.*a3);
C1=(a1.*a5+a2.*a4)./(a4+a1.*a3);
Q=C1.*cosh(M1.*y)+C2.*sinh(M1.*y)+(1./M12).*(Ao+A1.*y);
SF=M1.*(C1.*sinh(M1.*y)+C2.*cosh(M1.*y))+A1./(M1.^2);
Vfr=(C1./M1).*(sinh(M1))+(C2./M1).*(cosh(M1)-1)+(1./(M1.^2)).*(Ao+A1./2);
T=Ao+A1.*y;
Qr=real(Q);
Qm=imag(Q);
sfa0=-real(SF);
sf0=-imag(SF);
Vfrb=real(Vfr);
Vfrc=imag(Vfr);
xlabel('\betavKn','fontsize',11);
ylabel('\tau_{z1}','fontsize',11);
hold on
plot (y,Qr,'k','linestyle','-')
hold off
```

```
% Fully developed MHD natural convection in a vertical micro-porous channel
%with Hall Effect
clc;
h=0.001;
%y=1;
[y]=0:h:1;
M=2;
BvKn=0.05;
%BvKn=0:h:0.1;
ln=1.667;
zi=-1;
S=0.5;
Pr=0.71;
m=0.000;
M12=(M.^2)./(1+i.*m);
B=(1-zi)./(BvKn.*ln.*S.*Pr-1+exp(S.*Pr)+BvKn.*ln.*S.*Pr.*(S.*Pr));
A=zi+B.*(BvKn.*ln.*S.*Pr-1);
b1=S./2;
b2=((S.^2)./4)+M12;
b3=b1+sqrt(b2);
b4=b1-sqrt(b2);
b5=(B.*S.*Pr)./(S.^2.*Pr.^2-S.^2.*Pr-M12);
b6=((A./M12)-(B./(S.^2.*Pr.^2-S.^2.*Pr-M12)));
b7=BvKn.*b5;
b8=1-BvKn.*b3;
b9=b4.*BvKn-1;
b10=-b7-b6;
b11=((A./M12)-((B.*exp(S.*Pr))./(S.^2.*Pr.^2-S.^2.*Pr-M12)));
b12=BvKn.*b5.*exp(S.*Pr);
b13=exp(b3)+BvKn.*b3.*exp(b3);
b14=exp(b4)+BvKn.*b4.*exp(b4);
b15=b12-b11;
C2=(b15.*b8-b10.*b13)./(b9.*b13+b14.*b8);
C1=(C2.*b9+b10)./b8;
Q=C1.*exp(b3.*y)+C2.*exp(b4.*y)+A./M12-(B.*exp(S.*Pr.*y))./(S.^2.*Pr.^2-S.^2.*Pr-M12);
T=A+B.*exp(S.*Pr.*y);
SF=C1.*b3.*exp(b3.*y)+C2.*b4.*exp(b4.*y)-b5.*exp(S.*Pr.*y);
Ma=C1./b3.*(exp(b3)-1)+C2./b4.*(exp(b4)-1)+A./M12-(b5./(S.^2.*Pr.^2)).*(exp(S.*Pr)-1);
Qs=real(Q);
Qss=imag(Q);
Sk=real(SF);
Si=imag(SF);
vu=real(Ma);
```

```
vw=imag(Ma);
box on
xlabel('y','fontsize',11);
ylabel('velocity (w)','fontsize',11);
hold on
plot (y,Qs,'k','linestyle','-')
hold off
```